

UDC 624.014

## SEARCHING FOR SHEAR FORCES FLOWS IN ARBITRARY CROSS-SECTIONS OF THIN-WALLED BARS: NUMERICAL ALGORITHM AND SOFTWARE IMPLEMENTATION

V.V. Yurchenko,

Cand. Of Tech. Sc., Assoc. Prof.

*Kyiv National University of Civil Engineering and Architecture  
Povitroflotskyj av., 31, Kyiv, 03680*

The problem of shear stresses outside longitudinal edges of an arbitrary cross-section (including open-closed multi-contour cross-sections) of a thin-walled bar subjected to the general load case has been considered in the paper. The formulated problem has been reduced to the searching problem for unknown shear forces flows that have the least value of the Castigliano's functional. Besides, constraints-equalities of shear forces flows equilibrium formulated for cross-section branch points, as well as equilibrium equation formulated for the whole cross-section relating to longitudinal axes of the thin-walled bar have been taken into account.

A detailed numerical algorithm intended to solve the formulated problem has been proposed by the paper. Developed algorithm has been implemented in SCAD Office environment by the program TONUS. Numerical examples for calculation of thin-walled bars with open and open-closed multi-contour cross-sections have been considered in order to validate developed algorithm and verify calculation accuracy for sectorial cross-section geometrical properties and shear stresses caused by warping torque and shear forces.

**Keywords:** thin-walled bar, arbitrary cross-section, shear forces flow, closed contour, graph theory, Castigliano's functional, mathematical programming task, method of Lagrange multipliers, algorithm, software implementation

**Introduction.** To provide desired stiffness and strength in torsion bridge superstructures are often constructed with a cross-section consisting of multiple cells which have thin walls relative to their overall dimensions. When the cross-section contains multiple cells they all contribute resistance to applied torsion and for elastic continuity each cell must twist the same amount. With these considerations, equilibrium and compatibility conditions allow simultaneous equations to be formed and solved to determine the shear flow for each cell [1].

R.K. Dowell and T.P. Johnson proposed a relaxation method that distributes incremental shear flows back and forth between cells, reducing errors with each distribution cycle, until the final shear flows for all cells approximate the correct values [1]. In this paper, a closed-form approach has been introduced to determine, exactly, both the torsional constant and all shear flows for multi-cell cross-sections under torsion.

The problem of shear stresses determination for thin-walled bars has been also studied by V. Slivker in [2, 3] for the general loading case. His semi-sheared theory has been applied by Lalin V.V. et al. [4] for the stability problems of thin-walled bars.

Further investigations in this area require the development of a detailed algorithm intended to software implementation in a computer-aided design system for thin-walled bar structures [5]. Such algorithm can be validated

against benchmark examples as well as finite element results [6]. It is reasonable to construct this algorithm using the mathematical apparatus of the graph theory as it is convenient mathematical apparatus to describe the topological properties of multi-cellular cross-section.

The graph algorithm used in this paper is given first by Tarjan [7]. Its application in analysis of thin-walled multi-cellular section is described by Alfano et al. [8], but the distribution of torsion stresses due to a change in normal stresses has not been considered. The graph theory has been also applied in [9, 10] to calculate the geometrical cross-sectional properties of thin-walled bars with hybrid (open-closed) types of cross-sections.

Simple digital computer program has been created to evaluate the bending shear flow of any multiply-connected cellular sections has been developed by Chai H. Yoo et al. [11]. Prokić has developed a computer program for the determination of the torsional and flexural properties of thin-walled beams with arbitrary open-closed cross-section [12]. In his paper graph theory has been also applied to establish the topological properties of multi-cellular cross-section. Gurujee C.S. and Shah K.R. [13] presented a general purpose computer program capable of analyzing any planar frame made up of bar members which can be categorized as thin-walled structural members. G.K.Choudhary and K.M. Doshi proposed an algorithm for shear stress evaluation in ship hull girders [14].

Though many papers are written on behavior of thin-walled bars development of a general computer program for the design and verification of thin-walled bar structural members remains an actual task. Despite the prevailing influence of normal stresses on the stress-strain state of thin-walled bars design and verification of thin-walled structural members should be performed taking into account not only normal stresses, but also shear stresses. Therefore, in the paper a thin-walled bar of an arbitrary cross-section which is undergone to the general load case is considered as *investigated object*. The main *research question* is development of mathematical support and knoware for numerical solution for shear stresses problem with orientation on software implementation in a computer-aided design system for thin-walled bar structures.

**1. Problem formulation.** Let us consider the problem of shear stresses on longitudinal edges of an arbitrary section of a thin-walled bar that can consist of several closed (connected and/or disconnected) contours and/or also open parts. Let us introduce on the plane of thin-walled cross-section a Cartesian coordinate system  $y_c O z_c$  with the origin in the center of mass  $C$  of the section, the direction of the coordinate system axes  $y_c O z_c$  coincides with the direction of principle axes of inertia. Let us also introduce on the plane of thin-walled cross-section a Cartesian coordinate system  $y_s O z_s$  with the origin in the shear center  $S$  of the section, the direction of the coordinate system axes  $y_s O z_s$  coincides with the direction of principle axes of inertia (Fig. 1).

Let us introduce in further consideration the system of angular position coordinate with the origin in certain (generally randomly selected) sectional point. Each considered sectional point can be associated with the angular position  $\zeta$ . The value  $\zeta$  should be calculated as the geometrical length of the

curve constructed from the origin to the considered sectional point taken along the sectional contour. We also assume that the increment of the angular position  $\zeta$  corresponds to the positive direction of section path tracing.

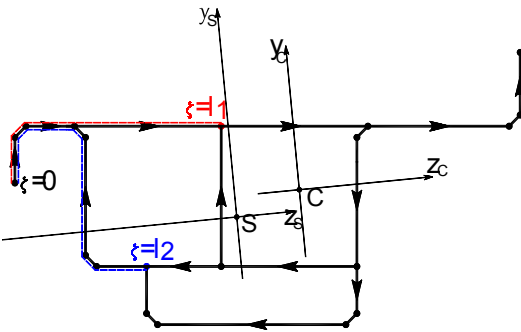


Fig. 1. Cross-section of a thin-walled bar with representation of different angular positions as examples

We assume that the integral geometrical properties of the section are known:  $A$  is the cross-sectional area,  $I_y$  and  $I_z$  are the second moments of area relative to the main axes of inertia which coincide with axes of global Cartesian coordinate system  $y_c O z_c$ ;  $I_\omega$  is the sectorial moment of inertia;  $I_t$  is the second moment of area for pure torsion. We

also assume that the Young’s modulus  $E$  and the shear modulus  $G$  are constants for the whole cross-section of the thin-walled bar.

Generally, a thin-walled bar is subjected to the action of eight force factors. Axial force  $N$ , bending moments  $M_y$  and  $M_z$  relative to the principle axes of inertia and warping bimoment  $B$  are applied at the center of mass  $C$  (see Fig. 1) of the section and cause normal stresses in the cross-section  $\sigma_i(x, \zeta)$ :

$$\sigma_i(x, \zeta) = \frac{N(x)}{A} + \frac{M_y(x)}{I_y} z_i(\zeta) + \frac{M_z(x)}{I_z} y_i(\zeta) + \frac{B(x)}{I_\omega} \varpi_i(\zeta), \tag{1.1}$$

where  $y_i(\zeta)$ ,  $z_i(\zeta)$ ,  $\varpi_i(\zeta)$  are coordinates and sectorial coordinate of the considered point in cross-section of a thin-walled bar.

Shear forces  $Q_y$  and  $Q_z$ , total torque  $M_x$  and warping torque  $M_\omega$  are applied at the shear center  $S$  (see Fig. 1) of the cross-section and cause shear stresses in the cross-section, which can be written in terms of shear forces flows  $T_j(x, \zeta)$  as presented below:

$$\tau_j(x, \zeta) = \frac{T_j(x, \zeta)}{\delta_j(\zeta)}, \tag{1.2}$$

where  $\delta_j(\zeta)$  is the thickness of considered  $j^{\text{th}}$  section element.

An arbitrary section of a thin-walled bar can be described by the set of sectional points  $\mathbf{P} = \{ \vec{p}_p = \{ y_p, z_p \} \mid p = \overline{1, n_p} \}$  ( $y_p$  and  $z_p$  are the coordinates of  $p^{\text{th}}$  sectional point in the global Cartesian coordinate system  $y_c O z_c$ ) and by the set of sectional segments  $\mathbf{S} = \{ \vec{s}_s = \{ p_s^{st}, p_s^{end} \} \mid s = \overline{1, n_s} \}$ , which connect

some two adjacent sectional points (see Fig. 2), where  $n_p$  and  $n_s$  are the numbers of the sectional points and segments accordingly.

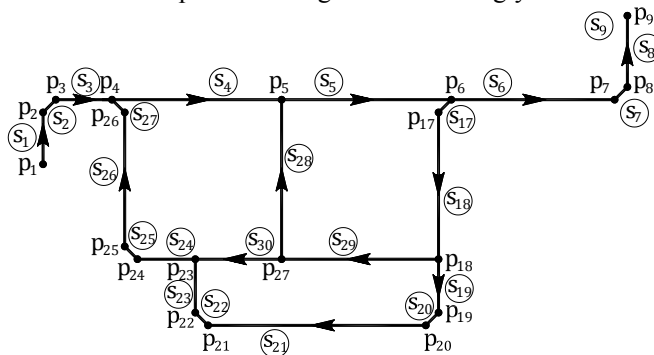


Fig. 2. Arbitrary cross-section of a thin-walled bar determined on the set of sectional points  $P$  and set of sectional segments  $S$

Specified segment thickness  $\delta = \{\delta_s | s = \overline{1, n_s}\}$  corresponds to each sectional segment. The set of sectorial coordinates  $\omega = \{\omega_p | p = \overline{1, n_p}\}$  and the set of normalized sectorial coordinates  $\bar{\omega} = \{\bar{\omega}_p | p = \overline{1, n_p}\}$  of the section correspond to the set of the sectional points  $P$ , assuming that the values of the sectorial coordinates and normalized sectorial coordinates in each cross-sectional point are known [17, 18].

The set of angular positions  $\zeta = \{\zeta_\kappa = \{\zeta_\kappa^{start}, \zeta_\kappa^{end}\} | \kappa = \overline{1, n_\zeta - 1}\}$  is actually intended to implement a numerical integration taken along the thin-walled section contour (for example, when calculating geometrical properties of the cross-section, values of shear forces flows, etc.), where  $\kappa$  is the number of segment,  $n_\zeta - 1$  is the number of sectional segments. It should be noted that the angular positions are attributes of the ends of the sectional segments.

The initial data about the thin-walled section should be mapped onto the set of the angular positions  $\zeta$ ,  $\kappa = \overline{1, n_\zeta - 1}$ , by means of corresponding sets of sectional segments  $S^\zeta = \{s_\kappa^\zeta = \{\zeta_\kappa^{start}, \zeta_\kappa^{end}\} : \zeta_\kappa^{start}, \zeta_\kappa^{end} \subseteq \zeta\}$ , set of sectorial coordinates  $\omega^\zeta = \{\bar{\omega}_\kappa^\zeta = \{\omega_\kappa^{start}, \omega_\kappa^{end}\} : \omega_\kappa^{start}, \omega_\kappa^{end} \subseteq \omega\}$  for the ends of sectional segments as well as the set of thicknesses  $\delta^\zeta = \{\delta_\kappa^\zeta \subseteq \delta\}$  for the segments,  $\kappa = \overline{1, n_\zeta - 1}$ .

**2. Construction of connected graph  $G$  associated with a section of a thin-walled bar.** An arbitrary cross-section of a thin-walled bar can be associated with a planar connected non-oriented graph  $G$  determined on the sets of  $G = \{V, R\}$ , where  $V$  is the finite set of the graph vertices,  $R$  is the set of the graph edges or the set of unordered pairs on  $V$  (see Fig. 3) [15, 16].

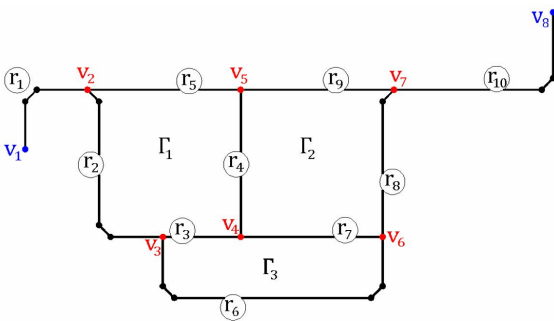


Fig 3. Graph  $G$  associated with cross-section of thin-walled bar ( $v_2 \dots v_7$  – branch points,  $v_1, v_8$  – end points)

Herewith, for each graph edge  $r = \{u, v\} \in R$  we assume that  $u \neq v$ .

The vertices of the graph  $G$  are associated with characteristic sectional points only, which can be either:

1) branch points are sectional points connected with more than two sectional

segments,  $v^p = \{\vec{p}_v \mid v = \overline{1, n_v}\}$ , here  $n_v$  is the number of these points;

2) end points are sectional points connected with only one sectional segment  $v^p_{end} = \{\vec{p}_g \mid g = \overline{1, n_g}\}$ , here  $n_g$  is the number of these points.

The edges of the graph  $G$  are associated with sectional parts located between characteristic sectional points (with unbranched sectional parts). An edge of the graph  $G$ , as a rule, may contain several sectional segments, so the full information about edge  $R_j^S$  of the graph can be described by the set of sectional

segments  $\vec{s}_r^S, r = \overline{1, n_{r_j}}$ , from the array  $S^S = \{\vec{s}_\kappa^S = \{\zeta_\kappa^{start}, \zeta_\kappa^{end}\} \mid \kappa = \overline{1, n_S - 1}\}$ ,  $\vec{s}_r^S \in S^S$ , belonging to considered graph edge,  $\vec{s}_r^S \in R_j$ :  $R_j^S = \{\vec{s}_r^S \mid \vec{s}_r^S \in S^S \wedge \vec{s}_r^S \in R_j \mid r = \overline{1, n_{r_j}}\}$ , here  $n_{r_j}$  is the number of segments for  $j^{th}$  graph edge. The set of all the graph edges defined on the set of segments  $S^S$  can be expressed as  $R^S = \{R_j^S \mid j = \overline{1, n_r}\}$ .

We also assume that the arbitrary section of the thin-walled bar may contain some quantity of closed contours. Each closed contour is associated with a cycle of the graph  $G$  or with a vertices sequence  $v_0^k, v_1^k, v_2^k, \dots, v_n^k$ , such that  $v_i^k \mapsto v_{i+1}^k \forall i \Leftrightarrow \exists v_{i+1}^k$ , where  $n_k$  is the number of closed contours in the section (the number of the graph  $G$  cycles).

Some closed contour of a section  $\Gamma_k^{r^S}$  (a basic cycle of the graph  $G$ ) can be definitely determined by the set of the graph edges  $R_j^S \in R^S$  belonging to the considered contour  $\Gamma_k^{r^S} = \{R_j^S \mid j = \overline{1, n_{r^S \Gamma_k}}\}$ , where  $n_{r^S \Gamma_k}$  is the number of the graph edges belonging to  $k^{th}$  closed contour. Besides, it is convenient to have the mapping of the closed contour  $\Gamma_k^{r^S}$  onto the set of sectional segments  $\vec{s}_m^S, \vec{s}_m^S \in S^S$ , belonging to the considered closed contour,  $\forall m = \overline{1, n_{S \Gamma_k}}$ :

$\Gamma_k^\zeta = \left\{ \vec{s}_m^\zeta : \vec{s}_m^\zeta \in \mathbf{S}^\zeta, \exists \mathbf{R}_\alpha^\zeta \subseteq \mathbf{R}^\zeta : \vec{s}_m^\zeta \subseteq \mathbf{R}_\alpha^\zeta \wedge \mathbf{R}_\alpha^\zeta \subseteq \Gamma_k^{r\zeta} \right\}$ , here  $n_{\zeta\Gamma_k}$  is the number of the sectional segments belonging to  $k^{\text{th}}$  closed contour.

The closed contours (basic cycles of the graph  $\mathbf{G}^\zeta$ ) defined on the set of graph edges  $\mathbf{R}^\zeta$  and on the set of section segments  $\mathbf{S}^\zeta$  can be described as  $\Phi^{r\zeta} = \left\{ \Gamma_k^{r\zeta} \mid k = \overline{1, n_k} \right\}$  and  $\Phi^\zeta = \left\{ \Gamma_k^\zeta \mid k = \overline{1, n_k} \right\}$  accordingly. It should be noted that the identification of closed contours in the section  $\Phi^{r\zeta}$  and  $\Phi^\zeta$  can be easily implemented using depth-first search algorithms on the graph.

Let us compose an incidence matrix  $\mathbf{I}$  for the graph  $\mathbf{G}^\zeta$  with dimensions  $n_v \times n_r$ ,  $\mathbf{I} = \left\{ g_{ij} \mid i = \overline{1, n_v}, j = \overline{1, n_r} \right\}$ . The components of the matrix take the following values:  $g_{ij} = 1$ , if  $i^{\text{th}}$  graph vertex is a start vertex for  $j^{\text{th}}$  edge;  $g_{ij} = -1$ , if  $i^{\text{th}}$  graph vertex is an end vertex for  $j^{\text{th}}$  edge;  $g_{ij} = 0$ , otherwise. Let us also introduce a matrix  $|\mathbf{I}| = \left\{ |g_{ij}| \mid i = \overline{1, n_v}, j = \overline{1, n_r} \right\}$  composed of the modulus of elements  $g_{ij}$  of the matrix  $\mathbf{I}$ .

Next, we can compose a matrix of basic graph cycles  $\mathbf{F}$  with dimensions  $n_k \times n_r$ ,  $\mathbf{F} = \left\{ f_{kj} \right\}, k = \overline{1, n_k}, j = \overline{1, n_r}$ . The components of the matrix take the following values:  $f_{kj} = 1$ , if  $j^{\text{th}}$  graph edge belongs to  $k^{\text{th}}$  basic graph cycle ( $\mathbf{R}_j^\zeta \subseteq \Gamma_k^\zeta$ ) and the edge direction coincides with the positive direction of path tracing;  $f_{kj} = -1$ , if  $j^{\text{th}}$  graph edge belongs to  $k^{\text{th}}$  basic graph cycle ( $\mathbf{R}_j^\zeta \subseteq \Gamma_k^\zeta$ ) and the edge direction does not coincide with the positive direction of path tracing;  $f_{kj} = 0$ , if  $j^{\text{th}}$  graph edge does not belong to  $k^{\text{th}}$  basic graph cycle ( $\mathbf{R}_j^\zeta \cap \Gamma_k^\zeta = \emptyset$ ).

### 3. Resolving equations relating to distribution of shear forces flows taken along closed contours for an arbitrary section of a thin-walled bar.

Each  $j^{\text{th}}$  edge  $\mathbf{R}_j^\zeta$ ,  $j = \overline{1, n_r}$  of the graph  $\mathbf{G}^\zeta$  corresponds to a constant – edge weight,  $\forall \kappa : \vec{s}_\kappa^\zeta \in \mathbf{R}_j^\zeta \wedge \vec{s}_\kappa^\zeta \in \mathbf{S}^\zeta$ :

$$p_j = \int_{\ell_{vj}} \frac{d\zeta}{\delta(\zeta)} = \sum_{r=1}^{n_{\zeta r j}} \int_{\ell_\zeta \in \mathbf{R}_j^\zeta} \frac{d\zeta}{\delta(\zeta)} = \sum_{r=1}^{n_{\zeta r j}} \frac{1}{\delta_\kappa^\zeta} \int_{\zeta_\kappa}^{\zeta_{\kappa+1}} d\zeta = \sum_{r=1}^{n_{\zeta r j}} \frac{l_\kappa^\zeta}{\delta_\kappa^\zeta}. \quad (2.1)$$

Let us also compose the *weighting matrix of unbranched sectional parts* (edges of graph  $\mathbf{G}^\zeta$ ) – a square matrix  $\mathbf{W}$  with dimensions  $n_r \times n_r$  and diagonal elements  $p_j$ ,  $j = \overline{1, n_r}$ :

$$\mathbf{W} = \begin{bmatrix} p_1 & 0 & \dots & 0 \\ 0 & p_2 & \dots & 0 \\ \vdots & \vdots & \ddots & \vdots \\ 0 & 0 & 0 & p_{n_r} \end{bmatrix}. \tag{2.2}$$

Besides, each  $j^{\text{th}}$  graph edge  $\mathbf{R}_j^\zeta$  corresponds to the increment of the sectorial coordinate  $\Delta\omega_{r,j}^\zeta = \left\{ \Delta\omega_{r,j}^\zeta \mid j = \overline{1, n_r} \right\}^T$ ,  $\forall k : \vec{s}_k^\zeta \in \mathbf{R}_j^\zeta \wedge \vec{s}_k^\zeta \in \mathbf{S}^\zeta$ :

$$\Delta\omega_{r,j}^\zeta = \int_{\ell_{rj}} \rho d\zeta = \int_{\ell_{rj}} d\omega = \sum_{r=1}^{n_{\sigma j}} \int_{\ell_\zeta \in \mathbf{R}_j^\zeta} d\omega = \sum_{r=1}^{n_{\sigma j}} \int_{\zeta_k}^{\zeta_{k+1}} d\omega = \sum_{r=1}^{n_{\sigma j}} \Delta\omega_{r,j}^\zeta. \tag{2.3}$$

Each closed contour of the section  $\Gamma_k^{r\zeta}$ ,  $k = \overline{1, n_k}$ , corresponds to the following constant – *contour weight*,  $f_{kj} \in \mathbf{F}$ ,  $\forall j : \mathbf{R}_j^\zeta \subseteq \Gamma_k^{r\zeta}$ :

$$\tilde{p}_k = \oint_{\Gamma_k^{r\zeta}} \frac{d\zeta}{\delta(\zeta)} = \int_{\mathbf{R}_j^\zeta \subseteq \Gamma_k^{r\zeta}} \frac{d\zeta}{\delta(\zeta)} = \sum_{j=1}^{n_{r\zeta k}} |f_{kj}| p_j. \tag{2.4}$$

Let us also introduce the *weighting matrix of sectional contours* – a square matrix  $\mathbf{K}$  with dimensions  $n_k \times n_k$ :

$$\mathbf{K} = \begin{bmatrix} \tilde{P}_{11} & -p_{12} & \dots & -p_{1k} & \dots & -p_{1n_k} \\ -p_{21} & \tilde{P}_{22} & \dots & -p_{2k} & \dots & -p_{2n_k} \\ \vdots & \vdots & \ddots & \vdots & \ddots & \vdots \\ -p_{k1} & -p_{k2} & \dots & \tilde{P}_{kk} & \dots & -p_{kn_k} \\ \vdots & \vdots & \vdots & \vdots & \ddots & \vdots \\ -p_{n_k 1} & -p_{n_k 2} & \dots & -p_{n_k k} & \dots & \tilde{P}_{n_k n_k} \end{bmatrix}, \tag{2.5}$$

here the diagonal elements of the matrix are the weights of  $k^{\text{th}}$  closed contour,  $\tilde{p}_{kk} = \tilde{p}_k$ ,  $k = \overline{1, n_k}$ ; other elements of the matrix  $p_{\alpha\beta}$  take zero value  $p_{\alpha\beta} = p_{\beta\alpha} = 0$ , when corresponded closed contours have no common edges:  $\Gamma_\alpha^\zeta \cap \Gamma_\beta^\zeta = \emptyset$ , and the sum of the weights for all common edges:

$$p_{\alpha\beta} = p_{\beta\alpha} = \sum_r p_r, \forall r : \mathbf{R}_r^\zeta \subseteq \Gamma_\alpha^\zeta \wedge \mathbf{R}_r^\zeta \subseteq \Gamma_\beta^\zeta.$$

Let us consider the problem of torsion for an arbitrary thin-walled section subjected to total torque  $M_x$  only. When the cross-section consists of certain number of closed (connected and/or disconnected) contours, as well as open parts, the torsion problem for the cross-section of the thin-walled bar is statically indeterminate. That is why not only static equations but also strain compatibility conditions must be introduced to consideration.

Let us formulate the strain compatibility conditions considering Castigliano’s functional. The latter can be identified with an expression for strain energy formulated in terms of stresses for an isotropic material [3]:

$$C = \frac{1}{2G} \left( \sum_{j=1}^{n_r} \left( \int_{\ell_j} \frac{(\sigma(\zeta))^2}{2(1+\nu)} \delta(\zeta) d\zeta + \int_{\ell_j} (\tau(\zeta))^2 \delta(\zeta) d\zeta \right) \right). \tag{2.6}$$

Besides, normal stresses  $\sigma(\zeta)$  can be omitted, as total torque acts only:

$$C = \frac{1}{2G} \left( \sum_{j=1}^{n_r} \int_{\ell_j} (\tau(\zeta))^2 \delta(\zeta) d\zeta \right). \tag{2.7}$$

Let us rewrite Castigliano's functional  $C$  (2.7) substituting shear stresses  $\tau(\zeta)$  by their representation in terms of contour flows  $\vec{T} = \{\tilde{T}_k\}^T, k = \overline{1, n_k}$ :

$$\tilde{v}_k(\zeta) = \frac{\tilde{T}_k(\zeta)}{\delta_k(\zeta)}, \tag{2.8}$$

In this case we obtain the following expression for Castigliano's functional:

$$C = \frac{\tilde{T}_1^2}{2G} \oint_{\Gamma_1} \frac{d\zeta}{\delta(\zeta)} + \frac{\tilde{T}_2^2}{2G} \oint_{\Gamma_2} \frac{d\zeta}{\delta(\zeta)} + \dots + \frac{\tilde{T}_k^2}{2G} \oint_{\Gamma_k} \frac{d\zeta}{\delta(\zeta)} - \frac{\tilde{T}_1 \tilde{T}_2}{G} \int_{\Gamma_{12}} \frac{d\zeta}{\delta(\zeta)} - \frac{\tilde{T}_1 \tilde{T}_3}{G} \int_{\Gamma_{13}} \frac{d\zeta}{\delta(\zeta)} - \dots$$

$$\dots - \frac{\tilde{T}_1 \tilde{T}_k}{G} \int_{\Gamma_{1k}} \frac{d\zeta}{\delta(\zeta)} - \frac{\tilde{T}_2 \tilde{T}_3}{G} \int_{\Gamma_{23}} \frac{d\zeta}{\delta(\zeta)} - \frac{\tilde{T}_2 \tilde{T}_4}{G} \int_{\Gamma_{24}} \frac{d\zeta}{\delta(\zeta)} - \dots - \frac{\tilde{T}_2 \tilde{T}_k}{G} \int_{\Gamma_{2k}} \frac{d\zeta}{\delta(\zeta)} - \dots$$

$$\dots - \frac{\tilde{T}_{k-1} \tilde{T}_k}{G} \int_{\Gamma_{k-1,k}} \frac{d\zeta}{\delta(\zeta)}. \tag{2.9}$$

Negative summands  $\frac{\tilde{T}_{k-1} \tilde{T}_k}{G} \int_{\Gamma_{k-1,k}} \frac{d\zeta}{\delta(\zeta)}$  in (2.9) take into account the mutual

work of the counter flows of shear stresses on the common parts of the thin-walled bar cross-section.

It is evident that the resulting torsional moment in the section caused by all contour flows of shear stresses  $\vec{T} = \{\tilde{T}_k\}^T, k = \overline{1, n_k}$  equals to the sum of the torsional moments caused by each of these flows [3]:

$$M_x = \sum_{k=1}^{n_k} \tilde{T}_k \Omega_k, \tag{2.10}$$

here  $\Omega_k$  is the double area embraced by  $k^{\text{th}}$  closed contour  $\Gamma_k^\zeta$  of the section.

Let us present the formulated problem in the form of a mathematical programming task, namely as a problem for unknown contour shear forces flows  $\vec{T} = \{\tilde{T}_k\}^T, k = \overline{1, n_k}$  that ensure the least value of the optimum criterion, i.e. Castigliano's functional  $C$  (2.9) subject to equilibrium condition (2.10).

Let us present the solution of the formulated problem as follow:

$$\tilde{T}_k = \tilde{a}_k \frac{M_x}{\Omega_0}, \tag{2.11}$$



where  $\Omega_0$  is the double area for all closed contours of the section  $\Phi^s$ ,

$\Omega_0 = \sum_{k=1}^{n_k} \Omega_k$ ;  $\tilde{a}_k$  is the factor for the distribution of shear forces flows along  $k^{\text{th}}$  closed contour. Then Castigliano's functional (2.9) can be rewritten as presented below:

$$\begin{aligned}
 C = \frac{M_x^2}{2G\Omega_0^2} & \left( \tilde{a}_1^2 \oint_{\Gamma_1} \frac{d\zeta}{\delta(\zeta)} + \tilde{a}_2^2 \oint_{\Gamma_2} \frac{d\zeta}{\delta(\zeta)} + \dots + \tilde{a}_k^2 \oint_{\Gamma_k} \frac{d\zeta}{\delta(\zeta)} - 2\tilde{a}_1\tilde{a}_2 \int_{\Gamma_{12}} \frac{d\zeta}{\delta(\zeta)} - \right. \\
 & - 2\tilde{a}_1\tilde{a}_3 \int_{\Gamma_{13}} \frac{d\zeta}{\delta(\zeta)} - \dots - 2\tilde{a}_1\tilde{a}_k \int_{\Gamma_{1k}} \frac{d\zeta}{\delta(\zeta)} - 2\tilde{a}_2\tilde{a}_3 \int_{\Gamma_{23}} \frac{d\zeta}{\delta(\zeta)} - 2\tilde{a}_2\tilde{a}_4 \int_{\Gamma_{24}} \frac{d\zeta}{\delta(\zeta)} - \dots \\
 & \left. \dots - 2\tilde{a}_2\tilde{a}_k \int_{\Gamma_{2k}} \frac{d\zeta}{\delta(\zeta)} - \dots - 2\tilde{a}_{k-1}\tilde{a}_k \int_{\Gamma_{k-1,k}} \frac{d\zeta}{\delta(\zeta)} \right), \tag{2.12}
 \end{aligned}$$

and the equilibrium equation (2.10) can be presented by the following:

$$M_x = \sum_{k=1}^{n_k} \tilde{a}_k \frac{M_x}{\Omega_0} \Omega_k = \frac{M_x}{\Omega_0} \sum_{k=1}^{n_k} \tilde{a}_k \Omega_k,$$

or

$$\Omega_0 = \sum_{k=1}^{n_k} \tilde{a}_k \Omega_k. \tag{2.13}$$

So, the formulated problem can be presented as searching problem for unknown distribution factors  $\vec{a} = \{\tilde{a}_k\}^T$ ,  $k = \overline{1, n_k}$  of shear forces flows taken along closed contours of section that ensure the least value of Castigliano's functional  $C$  (2.12) subject to equilibrium condition (2.13).

The method of Lagrange multipliers can be used to reduce the problem (2.12) – (2.13) to the searching for a stationary point of the following modified functional  $\Lambda(\vec{a}, \lambda_a)$ , where  $\lambda_a$  is the Lagrange multiplier. Besides, the stationary conditions for the modified functional  $\Lambda(\vec{a}, \lambda_a)$  can be transformed to a system of linear algebraic equations with an order of  $n_k + 1$  presented below in the vector-matrix form:

$$\begin{bmatrix} \mathbf{K} & \vec{\Omega} \\ (\vec{\Omega})^T & 0 \end{bmatrix} \times \begin{bmatrix} \vec{a} \\ \lambda_a \end{bmatrix} = \begin{bmatrix} \mathbf{0}_k \\ \Omega_0 \end{bmatrix}, \tag{2.14}$$

where  $\vec{\Omega} = \{\Omega_k\}^T$ ,  $k = \overline{1, n_k}$  is the column vector of double areas embraced by the closed contours of the thin-walled bar. The resolving system of equations (2.14) to calculate distribution factors  $\vec{a}_k = \{\tilde{a}_k\}^T$ ,  $k = \overline{1, n_k}$  of shear forces flows along the closed contours of the section has been presented below:

$$\begin{bmatrix} \tilde{p}_{11} & -p_{12} & \cdots & -p_{1k} & \cdots & -p_{1n_k} & \Omega_1 \\ -p_{21} & \tilde{p}_{22} & \cdots & -p_{2k} & \cdots & -p_{2n_k} & \Omega_2 \\ \vdots & \vdots & \ddots & \vdots & \vdots & \vdots & \vdots \\ -p_{k1} & -p_{k2} & \cdots & \tilde{p}_{kk} & \cdots & -p_{kn_k} & \Omega_k \\ \vdots & \vdots & \vdots & \vdots & \ddots & \vdots & \vdots \\ -p_{n_k 1} & -p_{n_k 2} & \cdots & -p_{n_k k} & \cdots & \tilde{p}_{n_k n_k} & \Omega_{n_k} \\ \Omega_1 & \Omega_2 & \cdots & \Omega_k & \cdots & \Omega_{n_k} & 0 \end{bmatrix} \times \begin{bmatrix} \tilde{a}_1 \\ \tilde{a}_2 \\ \vdots \\ \tilde{a}_k \\ \vdots \\ \tilde{a}_{n_k} \\ \lambda_a \end{bmatrix} = \begin{bmatrix} 0 \\ 0 \\ \vdots \\ 0 \\ \vdots \\ 0 \\ \Omega_0 \end{bmatrix}, \quad (2.15)$$

where the diagonal elements of the matrix are the weights of  $k^{\text{th}}$  closed contour,  $\tilde{p}_{kk} = \tilde{p}_k$ ,  $k = \overline{1, n_k}$ ;  $\Omega_k$  is double area embraced by  $k^{\text{th}}$  closed contour  $\Gamma_k^\zeta$ ,  $\Omega_0 = \sum_{k=1}^{n_k} \Omega_k$ ;  $\lambda_a$  is the Lagrange multiplier. Other elements of the matrix  $p_{\alpha\beta}$  take zero value  $p_{\alpha\beta} = p_{\beta\alpha} = 0$  when corresponded closed contours have no common edges:  $\Gamma_\alpha^\zeta \cap \Gamma_\beta^\zeta = \emptyset$ , and the sum of weights for all common edges [3] is  $p_{\alpha\beta} = p_{\beta\alpha} = \sum_r p_r, \forall r : \mathbf{R}_r^\zeta \subseteq \Gamma_\alpha^\zeta \wedge \mathbf{R}_r^\zeta \subseteq \Gamma_\beta^\zeta$ .

The solution of the system of algebraic equations (2.15) returns the column vector of factors  $\vec{\tilde{a}}_k = \{\tilde{a}_k | k = \overline{1, n_k}\}$  for the distribution of shear forces flows along the closed contours of the section. Based on  $\vec{\tilde{a}}_k$ , we can generate the column vector of factors for the distribution of shear forces flows along the graph  $\mathbf{G}$  edges:  $\mathbf{A}_r = \{a_j | j = \overline{1, n_r}\}$ , where each element should be determined as:

$$a_j = \sum_{k=1}^{n_k} f_{kj} \tilde{a}_k, \quad f_{kj} \in \mathbf{F} \quad \forall j = \overline{1, n_r}. \quad (2.16)$$

Since every graph edge  $\mathbf{R}_j^\zeta, j = \overline{1, n_r}$ , is described by the set of sectional segments  $\vec{s}_r^\zeta \in \mathbf{S}^\zeta$  as:  $\mathbf{R}_j^\zeta = \{\vec{s}_r^\zeta : \vec{s}_r^\zeta \in \mathbf{S}^\zeta \wedge \vec{s}_r^\zeta \in \mathbf{R}_j | r = \overline{1, n_{rj}}\}$ , then it is possible to determine for each sectional segment  $\vec{s}_\kappa^\zeta \in \mathbf{S}^\zeta$  the value of piecewise constant *distribution function for shear flows taken along section*  $a^\zeta(\zeta)$  as the set of  $\mathbf{a}^\zeta = \{a_\kappa^\zeta | \kappa = \overline{1, n_\zeta - 1}\}$  as follows:  $a_\kappa^\zeta = a_j, \forall \kappa : \vec{s}_\kappa^\zeta \cap \mathbf{P}^\zeta \neq \emptyset$ , and  $a_\kappa^\zeta = 0$ , otherwise.

**3. Resolving equations for an arbitrary cross-section of a thin-walled bar.** The search problem of shear forces flows for an arbitrary cross-section of a thin-walled bar (including open-closed multi-contour cross-sections) can be transformed into a minimization problem of Castigliano's functional  $\mathbf{C}$  subject to constraints-equalities of shear forces flows equilibrium formulated for cross-section branch points as well as subject to equilibrium equation for the whole cross-section relating to longitudinal axes of the thin-walled bar [3].

Let us present the formulated problem as a mathematical programming task, namely as searching for unknown values of shear forces flows at the start points

of unbranched parts of a section:

$$\vec{T}_S = \{T_{S,j}\}^T, j = \overline{1, n_r}, \quad (3.1)$$

which ensure the least value of the optimum criterion – Castigliano’s functional  $\mathbf{C}$  :

$$\mathbf{C}^* = \mathbf{C}(\vec{T}_S^*) = \min_{\vec{T}_S \in \mathfrak{S}_T} \mathbf{C}(\vec{T}_S), \quad (3.2)$$

on a hyperplane of feasible decisions  $\mathfrak{S}_T$  described by the following system of constraints-equalities:

$$\begin{cases} \mathbf{f}(\vec{T}_S) = \{f_v(\vec{T}_S) = 0 \mid v = \overline{1, n_v - 1}\}; \\ f_x(\vec{T}_S) = 0; \end{cases} \quad (3.3)$$

where  $\vec{T}_S$  is the vector of design variables (searched shear flows);  $n_r$  is the number of unknown shear flows;  $\vec{T}_S^*$  is the optimum decision of the problem;  $\mathbf{C}^*$  is the minimum value of Castigliano’s functional;  $f_v$  is the function of the vector argument  $\vec{T}_S$ ;  $n_v$  is the general number of constraints-equalities  $f_v(\vec{T}_S)$  and  $f_x(\vec{T}_S)$  which define the hyperplane of feasible decisions  $\mathfrak{S}_T$  in the sought space.

For Castigliano’s functional  $\mathbf{C}$  we will consider Euler’s equations only which define the strain compatibility conditions and are expressed depending on shear forces flows  $\vec{T}_S = \{T_{S,j}\}^T, j = \overline{1, n_r}$ . Let us rewrite Castigliano’s functional  $\mathbf{C}$  Eq. (2.6) replacing normal stresses  $\sigma(\zeta)$  by Eq. (1.1), and shear stresses  $\tau(\zeta)$  – by the dependence on shear forces flows Eq. (1.2) as presented below:

$$\begin{aligned} \tau_j(\zeta) &= \frac{1}{\delta_j(\zeta)} \left( T_{S,j} - \frac{Q_z}{I_y} S_{oy,j}(\zeta) - \frac{Q_y}{I_z} S_{oz,j}(\zeta) - \frac{M_{\overline{\omega}}}{I_{\overline{\omega}}} S_{o\overline{\omega},j}(\zeta) \right), \quad (3.4) \\ \mathbf{C} &= \sum_{j=1}^{n_r} \left[ \frac{1}{2G} \int_{\ell_j} \frac{1}{2(1+\nu)} \left( \frac{N}{A} + \frac{M_y}{I_y} z_j + \frac{M_z}{I_z} y_j + \frac{B}{I_{\overline{\omega}}} \overline{\omega}_j \right)^2 \delta_j d\zeta + \right. \\ &+ \frac{1}{2G} \int_{\ell_j} \left( T_{S,j}^2 - 2T_{S,j} \frac{Q_z}{I_y} S_{oy,j} - 2T_{S,j} \frac{Q_y}{I_z} S_{oz,j} - 2T_{S,j} \frac{M_{\overline{\omega}}}{I_{\overline{\omega}}} S_{o\overline{\omega},j} \right) \frac{d\zeta}{\delta_j} + \\ &\left. + \frac{1}{2G} \int_{\ell_j} \left( \frac{Q_z}{I_y} S_{oy,j} + \frac{Q_y}{I_z} S_{oz,j} + \frac{M_{\overline{\omega}}}{I_{\overline{\omega}}} S_{o\overline{\omega},j} \right)^2 \frac{d\zeta}{\delta_j} \right], \quad (3.5) \end{aligned}$$

here we omitted the functional dependence on the angular position  $\zeta$  (to simplify presented formulas).

Let us leave in (3.5) those summands that depend on shear forces flows values  $\vec{T}_S = \{T_{S,j}\}^T, j = \overline{1, n_r}$ , and also denote by the symbol ... all other summands that are do not depend on the vector  $\vec{T}_S$ . In this way we have obtain the expression for Castigliano’s functional  $\mathbf{C}$  in terms of shear forces flows  $\vec{T}_S = \{T_{S,j}\}^T$  [3] as presented below:

$$C = \sum_{j=1}^{n_r} \left( \int_{\ell_j} \left( \frac{T_{S,j}^2}{2G} - T_{S,j} \frac{Q_z}{GI_y} S_{oy,j} - T_{S,j} \frac{Q_y}{GI_z} S_{oz,j} - T_{S,j} \frac{M_{\overline{\omega}}}{GI_{\overline{\omega}}} S_{o\overline{\omega},j} \right) \frac{d\zeta}{\delta_j} + \dots \right), \quad (3.6)$$

$$C = \sum_{j=1}^{n_r} \left[ \frac{T_{S,j}^2}{2G} \int_{\ell_j} \frac{d\zeta}{\delta_j} - T_{S,j} \frac{Q_z}{GI_y} \int_{\ell_j} S_{oy,j} \frac{d\zeta}{\delta_j} - T_{S,j} \frac{Q_y}{GI_z} \int_{\ell_j} S_{oz,j} \frac{d\zeta}{\delta_j} - T_{S,j} \frac{M_{\overline{\omega}}}{GI_{\overline{\omega}}} \int_{\ell_j} S_{o\overline{\omega},j} \frac{d\zeta}{\delta_j} + \dots \right]. \quad (3.7)$$

Where the integral  $\int_{\ell_j} \frac{d\zeta}{\delta_j}$  can be calculated according to (2.1), and the integrals  $\int_{\ell_j} S_{oy,j} \frac{d\zeta}{\delta_j}$ ,  $\int_{\ell_j} S_{oz,j} \frac{d\zeta}{\delta_j}$  and  $\int_{\ell_j} S_{o\overline{\omega},j} \frac{d\zeta}{\delta_j}$  – using following equations

(3.8), (3.9) and (3.10) accordingly presented below,  $\forall \kappa: \vec{s}_{\kappa}^{\zeta} \in \mathbf{R}^{\zeta} \wedge \vec{s}_{\kappa}^{\zeta} \in \mathbf{S}^{\zeta}$ :

$$S_{hz,j} = \int_{\ell_{rj}} \frac{S_{oz,j}^{\zeta}(\zeta) d\zeta}{\delta(\zeta)} = \sum_{\kappa=1}^{n_{zj}} \left( \frac{I_{\kappa}^{\zeta}}{6\delta_{\kappa}^{\zeta}} \left( S_{oz,\kappa}^{\zeta,start} + 4S_{oz,\kappa}^{\zeta,mid} + S_{oz,\kappa}^{\zeta,end} \right) \right); \quad (3.8)$$

$$S_{hy,j} = \int_{\ell_{rj}} \frac{S_{oy,j}^{\zeta}(\zeta) d\zeta}{\delta(\zeta)} = \sum_{\kappa=1}^{n_{yj}} \left( \frac{I_{\kappa}^{\zeta}}{6\delta_{\kappa}^{\zeta}} \left( S_{oy,\kappa}^{\zeta,start} + 4S_{oy,\kappa}^{\zeta,mid} + S_{oy,\kappa}^{\zeta,end} \right) \right); \quad (3.9)$$

$$S_{h\overline{\omega},j} = \int_{\ell_{rj}} \frac{S_{o\overline{\omega},j}^{\zeta}(\zeta) d\zeta}{\delta(\zeta)} = \sum_{\kappa=1}^{n_{\overline{\omega}j}} \left( \frac{I_{\kappa}^{\zeta}}{6\delta_{\kappa}^{\zeta}} \left( S_{o\overline{\omega},\kappa}^{\zeta,start} + 4S_{o\overline{\omega},\kappa}^{\zeta,mid} + S_{o\overline{\omega},\kappa}^{\zeta,end} \right) \right). \quad (3.10)$$

Let us define the following column vectors consisting of  $n_r$  elements,  $\forall j = \overline{1, n_r}$  (according to the number of edges of the graph  $\mathbf{G}^r$ ):

$$\vec{S}_{hz} = \begin{bmatrix} S_{hz,1} \\ S_{hz,2} \\ \vdots \\ S_{hz,n_r} \end{bmatrix}; \quad \vec{S}_{hy} = \begin{bmatrix} S_{hy,1} \\ S_{hy,2} \\ \vdots \\ S_{hy,n_r} \end{bmatrix}; \quad \vec{S}_{h\overline{\omega}} = \begin{bmatrix} S_{h\overline{\omega},1} \\ S_{h\overline{\omega},2} \\ \vdots \\ S_{h\overline{\omega},n_r} \end{bmatrix}. \quad (3.11)$$

Using the weighting matrix of unbranched sectional parts  $\mathbf{W}$  (2.2) introduced above as well as column vectors  $\vec{S}_{hz}$ ,  $\vec{S}_{hy}$  and  $\vec{S}_{h\overline{\omega}}$  presented above (3.11), we can rewrite Castigliano’s functional (3.7) as the following vector-matrix equation:

$$C = \frac{1}{2G} \vec{T}_S^T \mathbf{W} \vec{T}_S - \vec{T}_S^T \frac{Q_z}{GI_y} \vec{S}_{hz} - \vec{T}_S^T \frac{Q_y}{GI_z} \vec{S}_{hy} - \vec{T}_S^T \frac{M_{\overline{\omega}}}{GI_{\overline{\omega}}} \vec{S}_{h\overline{\omega}} + \dots \quad (3.12)$$

Next, for each section branch point we can develop an equation of shear forces flows equilibrium in terms of projections on the longitudinal axis of the thin-walled bar (Fig. 4). In order to obtain the general view for these equations (the system of equations by the number of branch points in the section), we can

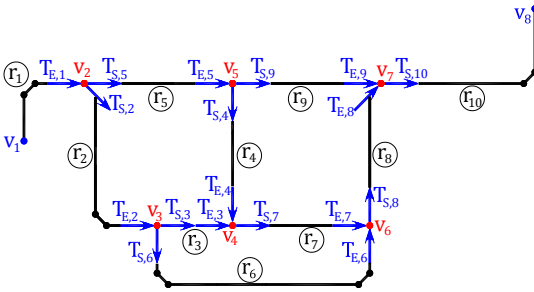


Fig. 4. Relating to formulate equilibrium equations for shear stresses flows in branch points of a thin-walled bar

use the incidence matrices  $\mathbf{i}$  and  $|\mathbf{i}|$  introduced above, which reflect the topological structure of the considered cross-section of the thin-walled bar. In this case we obtain the following system of equations presented below in the matrix-vector form:

$$\left( |\mathbf{i}| + \mathbf{i} \right) \vec{T}_S - \left( |\mathbf{i}| - \mathbf{i} \right) \vec{T}_E = \mathbf{0}, \tag{3.13}$$

where  $\vec{T}_S = \{T_{S,j}\}^T, j = \overline{1, n_r}$  is the vector of shear forces flows at the start points of unbranched sectional parts;  $\vec{T}_E = \{T_{E,j}\}^T, j = \overline{1, n_r}$  is the vector of shear forces flows at the end points of unbranched sectional parts:

$$\vec{T}_E = \vec{T}_S - \Delta \vec{T}, \tag{3.14}$$

where  $\Delta \vec{T} = \{\Delta T_j\}^T, j = \overline{1, n_r}$  is the vector of shear forces flows increments for each unbranched sectional part:

$$\Delta \vec{T}_j = \frac{Q_y}{I_z} \vec{S}_{z,j} + \frac{Q_z}{I_y} \vec{S}_{y,j} + \frac{M_{\omega}}{I_{\omega}} \vec{S}_{\omega,j}, \tag{3.15}$$

where the vectors  $\vec{S}_{z,j}, \vec{S}_{y,j}, \vec{S}_{\omega,j}$  are presented below:

$$\vec{S}_z = \begin{bmatrix} S_{z,1} \\ S_{z,2} \\ \vdots \\ S_{z,n_r} \end{bmatrix}; \quad \vec{S}_y = \begin{bmatrix} S_{y,1} \\ S_{y,2} \\ \vdots \\ S_{y,n_r} \end{bmatrix}; \quad \vec{S}_{\omega} = \begin{bmatrix} S_{\omega,1} \\ S_{\omega,2} \\ \vdots \\ S_{\omega,n_r} \end{bmatrix} \tag{3.16}$$

and the components of vectors  $\vec{S}_{z,j}, \vec{S}_{y,j}, \vec{S}_{\omega,j}$  can be calculated as follow,

$$\forall \kappa: \vec{s}_{\kappa}^{\zeta} \in \mathbf{R}^{\zeta} \wedge \vec{s}_{\kappa}^{\zeta} \in \mathbf{S}^{\zeta}:$$

$$S_{z,j} = \int_{\ell_{rj}} y^{\zeta}(\zeta) \delta(\zeta) d\zeta = \sum_{\kappa=1}^{n_{\zeta j}} \left( \delta_{\kappa}^{\zeta} I_{\kappa}^{\zeta} \left( y_{\kappa}^{\zeta, start} + \frac{1}{2} \Delta y_{\kappa}^{\zeta} \right) \right), \tag{3.17}$$

$$S_{y,j} = \int_{\ell_{rj}} z^{\zeta}(\zeta) \delta(\zeta) d\zeta = \sum_{\kappa=1}^{n_{\zeta j}} \left( \delta_{\kappa}^{\zeta} I_{\kappa}^{\zeta} \left( z_{\kappa}^{\zeta, start} + \frac{1}{2} \Delta z_{\kappa}^{\zeta} \right) \right), \tag{3.18}$$

$$S_{\omega,j} = \int_{\ell_{rj}} \omega^{\zeta}(\zeta) \delta(\zeta) d\zeta = \sum_{\kappa=1}^{n_{\zeta j}} \left( \delta_{\kappa}^{\zeta} I_{\kappa}^{\zeta} \left( \omega_{\kappa}^{\zeta, start} + \frac{1}{2} \Delta \omega_{\kappa}^{\zeta} \right) \right). \tag{3.19}$$

Let us rewrite the system of equations (3.13) substituting  $\vec{T}_E$  according to (3.14). We obtain the following system of equations:

$$\left(\|\mathbf{i}\| + \mathbf{i}\right)\vec{T}_S - \left(\|\mathbf{i}\| - \mathbf{i}\right) \times \left(\vec{T}_S - \Delta\vec{T}\right) = \mathbf{0}, \quad (3.20)$$

$$\left(\|\mathbf{i}\| + \mathbf{i}\right)\vec{T}_S - \left(\|\mathbf{i}\| - \mathbf{i}\right)\vec{T}_S + \left(\|\mathbf{i}\| - \mathbf{i}\right)\Delta\vec{T} = \mathbf{0}, \quad (3.21)$$

$$2\mathbf{i}\vec{T}_S + \left(\|\mathbf{i}\| - \mathbf{i}\right)\Delta\vec{T} = \mathbf{0} \quad (3.22)$$

and taking into account (3.15):

$$2\mathbf{i}\vec{T}_S + \left(\|\mathbf{i}\| - \mathbf{i}\right) \times \left( \frac{Q_y}{I_z} \vec{S}_{z,j} + \frac{Q_z}{I_y} \vec{S}_{y,j} + \frac{M_{\omega}}{I_{\omega}} \vec{S}_{\omega,j} \right) = \mathbf{0}. \quad (3.23)$$

The system of equations (3.23) presented above in the matrix-vector form has  $n_v$  equilibrium equations. The last equation is linear-dependent or a linear combination from the previous  $n_v - 1$  equations. Let us rewrite the system of equations (3.23) excluding the last equilibrium equation:

$$2\mathbf{i}'\vec{T}_S + \left(\|\mathbf{i}'\| - \mathbf{i}'\right) \times \left( \frac{Q_y}{I_z} \vec{S}_{z,j} + \frac{Q_z}{I_y} \vec{S}_{y,j} + \frac{M_{\omega}}{I_{\omega}} \vec{S}_{\omega,j} \right) = \mathbf{0}, \quad (3.24)$$

where  $\mathbf{i}'$  is the incidence matrix of the graph  $\mathbf{G}$  truncated by the last row with dimensions  $(n_v - 1) \times n_r$ ,  $\mathbf{i}' = \{g_{ij} \mid i = \overline{1, n_v - 1}, j = \overline{1, n_r}\}$ ;  $\|\mathbf{i}'\|$  is the matrix composed using the modulus of elements  $g_{ij}$  of the truncated matrix  $\mathbf{i}'$  as  $\|\mathbf{i}'\| = \{|g_{ij}| \mid i = \overline{1, n_v - 1}, j = \overline{1, n_r}\}$ .

It is possible to derive the last equilibrium equation relating to the longitudinal axis  $x-x$  of the thin-walled bar as a condition of the static equivalence of the torsion moment caused by the shear forces flows to the total torque  $M_x$  acting in the cross-section of the thin-walled bar:

$$M_x - \sum_{j=1}^{n_r} \int T_j(\zeta) d\omega = 0, \quad (3.25)$$

where  $T_j(\zeta)$  is the shear forces flow at some point of the cross-section, which can be expressed depending on shear forces flow  $T_{S,j}(\zeta)$  at the start point of the corresponded unbranched part of the section as follow:

$$T_j = T_{S,j} - \frac{Q_y}{I_z} S_{oz,j} - \frac{Q_z}{I_y} S_{oy,j} - \frac{M_{\omega}}{I_{\omega}} S_{o\omega,j}, \quad (3.26)$$

where we omitted the functional dependence from the angular position  $\zeta$  (to simplify presented formulas).

Then:

$$M_x - \sum_{j=1}^{n_r} \int \left( T_{S,j} - \frac{Q_y}{I_z} S_{oz,j} - \frac{Q_z}{I_y} S_{oy,j} - \frac{M_{\omega}}{I_{\omega}} S_{o\omega,j} \right) \rho d\zeta = 0;$$

$$M_x - \sum_{j=1}^{n_r} \left( T_{S,j} \int_{\ell_j} \rho d\zeta - \frac{Q_y}{I_z} \int_{\ell_j} S_{oz,j} \rho d\zeta - \frac{Q_z}{I_y} \int_{\ell_j} S_{oy,j} \rho d\zeta - \frac{M_{\overline{\omega}}}{I_{\overline{\omega}}} \int_{\ell_j} S_{o\overline{\omega},j} \rho d\zeta \right) = 0.$$

Finally, we obtain [3]:

$$\begin{aligned} & \sum_{j=1}^{n_r} T_{S,j} \int_{\ell_j} \rho d\zeta - \frac{Q_y}{I_z} \sum_{j=1}^{n_r} \int_{\ell_j} S_{oz,j} \rho d\zeta - \frac{Q_z}{I_y} \sum_{j=1}^{n_r} \int_{\ell_j} S_{oy,j} \rho d\zeta - \\ & - \frac{M_{\overline{\omega}}}{I_{\overline{\omega}}} \sum_{j=1}^{n_r} \int_{\ell_j} S_{o\overline{\omega},j} \rho d\zeta - M_x = 0, \end{aligned} \tag{3.27}$$

where integrals  $\sum_{j=1}^{n_r} \int_{\ell_j} S_{oz,j} \rho d\zeta$ ,  $\sum_{j=1}^{n_r} \int_{\ell_j} S_{oy,j} \rho d\zeta$  and  $\sum_{j=1}^{n_r} \int_{\ell_j} S_{o\overline{\omega},j} \rho d\zeta$  can be calculated using (3.28), (3.29) and (3.30) accordingly as presented below,  $\forall \kappa : \vec{s}_{\kappa}^{\zeta} \in \mathbf{R}_j^{\zeta} \wedge \vec{s}_{\kappa}^{\zeta} \in \mathbf{S}^{\zeta}$ :

$$S_{\rho z} = \sum_{j=1}^{n_r} \int_{\ell_{rj}} S_{oz,j}^{\zeta}(\omega) \rho d\zeta = \sum_{j=1}^{n_r} \left( \sum_{\kappa=1}^{n_{zj}} \frac{\Delta \omega_{\kappa}^{\zeta}}{6} \left( S_{oz,\kappa}^{\zeta, start} + 4S_{oz,\kappa}^{\zeta, mid} + S_{oz,\kappa}^{\zeta, end} \right) \right), \tag{3.28}$$

$$S_{\rho y} = \sum_{j=1}^{n_r} \int_{\ell_{rj}} S_{oy,j}^{\zeta}(\omega) \rho d\zeta = \sum_{j=1}^{n_r} \left( \sum_{\kappa=1}^{n_{zj}} \frac{\Delta \omega_{\kappa}^{\zeta}}{6} \left( S_{oy,\kappa}^{\zeta, start} + 4S_{oy,\kappa}^{\zeta, mid} + S_{oy,\kappa}^{\zeta, end} \right) \right), \tag{3.29}$$

$$S_{\rho \overline{\omega}} = \sum_{j=1}^{n_r} \int_{\ell_{rj}} S_{o\overline{\omega},j}^{\zeta}(\omega) \rho d\zeta = \sum_{j=1}^{n_r} \left( \sum_{\kappa=1}^{n_{zj}} \frac{\Delta \omega_{\kappa}^{\zeta}}{6} \left( S_{o\overline{\omega},\kappa}^{\zeta, start} + 4S_{o\overline{\omega},\kappa}^{\zeta, mid} + S_{o\overline{\omega},\kappa}^{\zeta, end} \right) \right). \tag{3.30}$$

Let us rewrite the constraints-equality (3.27) using vector representation taking into account equations (3.28), (3.29) and (3.30) as presented below:

$$\vec{\omega}^T \vec{T}_S - \frac{Q_y}{I_z} S_{\rho z} - \frac{Q_z}{I_y} S_{\rho y} - \frac{M_{\overline{\omega}}}{I_{\overline{\omega}}} S_{\rho \overline{\omega}} - M_x = 0. \tag{3.31}$$

Thus, the formulated problem is presented as a mathematical programming task of searching for the unknown values of shear forces flows at the start points of the unbranched parts of the section:

$$\vec{T}_S = \{T_{S,j}\}^T, j = \overline{1, n_r}, \tag{3.32}$$

which ensure the least value of the following Castigliano's functional **C** (3.12):

$$\mathbf{C} = \frac{1}{2G} \vec{T}_S^T \mathbf{W} \vec{T}_S - \vec{T}_S^T \frac{Q_y}{GI_z} \vec{S}_{hz} - \vec{T}_S^T \frac{Q_z}{GI_y} \vec{S}_{hy} - \vec{T}_S^T \frac{M_{\overline{\omega}}}{GI_{\overline{\omega}}} \vec{S}_{h\overline{\omega}} + \dots \rightarrow \min, \tag{3.33}$$

subject to the following equilibrium conditions (3.24) and (3.31):

$$\begin{cases} 2\mathbf{i}' \vec{T}_S + (|\mathbf{i}'| - \mathbf{i}') \left( \frac{Q_y}{I_z} \vec{S}_{z,j} + \frac{Q_z}{I_y} \vec{S}_{y,j} + \frac{M_{\overline{\omega}}}{I_{\overline{\omega}}} \vec{S}_{\overline{\omega},j} \right) = \mathbf{0}; \\ \vec{\omega}^T \vec{T}_S - \frac{Q_y}{I_z} S_{\rho z} - \frac{Q_z}{I_y} S_{\rho y} - \frac{M_{\overline{\omega}}}{I_{\overline{\omega}}} S_{\rho \overline{\omega}} - M_x = 0. \end{cases} \tag{3.34}$$

The method of Lagrange multipliers can be used to reduce the mathematical programming task (3.32) – (3.34) to the searching for the stationary point of the following modified functional  $\Lambda(\vec{T}_S, \vec{\lambda}^T, \lambda_{n_v})$ :

$$\begin{aligned} \Lambda(\vec{T}_S, \vec{\lambda}^T, \lambda_{n_v}) = & \frac{1}{2G} \vec{T}_S^T \mathbf{W} \vec{T}_S - \vec{T}_S^T \frac{Q_y}{GI_z} \vec{S}_{hz} - \vec{T}_S^T \frac{Q_z}{GI_y} \vec{S}_{hy} - \vec{T}_S^T \frac{M_{\overline{\omega}}}{GI_{\overline{\omega}}} \vec{S}_{h\overline{\omega}} + \\ & + \vec{\lambda}^T \left[ 2\mathbf{i}'^T \vec{T}_S + (|\mathbf{i}'| - \mathbf{i}') \left( \frac{Q_y}{I_z} \vec{S}_{z,j} + \frac{Q_z}{I_y} \vec{S}_{y,j} + \frac{M_{\overline{\omega}}}{I_{\overline{\omega}}} \vec{S}_{\overline{\omega},j} \right) \right] + \\ & + \lambda_{n_v} \left[ \vec{\omega}^T \vec{T}_S - \frac{Q_y}{I_z} S_{\rho z} - \frac{Q_z}{I_y} S_{\rho y} - \frac{M_{\overline{\omega}}}{I_{\overline{\omega}}} S_{\rho \overline{\omega}} - M_x \right] \rightarrow \min, \end{aligned} \quad (3.35)$$

where  $\vec{\lambda} = \{\lambda_f\}$ ,  $f = \overline{1, n_v - 1}$  is the vector of Lagrange multipliers consisting of  $n_v - 1$  elements;  $\lambda_{n_v}$  is an additional Lagrange multiplier.

The stationary conditions of the modified functional  $\Lambda(\vec{T}_S, \vec{\lambda}^T, \lambda_{n_v})$  (3.35) can be transformed into a system of  $n_r + n_v$  linear algebraic equations and presented in vector-matrix form as follow [3]:

$$\begin{aligned} & \begin{bmatrix} \frac{1}{G} \mathbf{W} & 2\mathbf{i}'^T & \Delta \omega_{\mathbf{r}}^{\xi} \\ 2\mathbf{i}' & \Theta_{n_v-1, n_v-1} & \mathbf{0}_{n_v-1} \\ (\Delta \omega_{\mathbf{r}}^{\xi})^T & \mathbf{0}_{n_v-1}^T & 0 \end{bmatrix} \times \begin{bmatrix} \vec{T}_S \\ \vec{\lambda} \\ \lambda_{n_v} \end{bmatrix} = M_x \times \begin{bmatrix} \mathbf{0}_{n_r} \\ \mathbf{0}_{n_v-1} \\ 1 \end{bmatrix} + \\ & + \frac{Q_y}{I_z} \times \begin{bmatrix} \vec{S}_{hz} \\ \frac{G}{S_{\rho z}} (\mathbf{i}' - |\mathbf{i}'|) \vec{S}_z \end{bmatrix} + \frac{Q_z}{I_y} \times \begin{bmatrix} \vec{S}_{hy} \\ \frac{G}{S_{\rho y}} (\mathbf{i}' - |\mathbf{i}'|) \vec{S}_y \end{bmatrix} + \frac{M_{\overline{\omega}}}{I_{\overline{\omega}}} \times \begin{bmatrix} \vec{S}_{h\overline{\omega}} \\ \frac{G}{S_{\rho \overline{\omega}}} (\mathbf{i}' - |\mathbf{i}'|) \vec{S}_{\overline{\omega}} \end{bmatrix}, \end{aligned} \quad (3.36)$$

where

$$\mathbf{M} = \begin{bmatrix} \frac{1}{G} \mathbf{W} & 2\mathbf{i}'^T & \Delta \omega_{\mathbf{r}}^{\xi} \\ 2\mathbf{i}' & \Theta_{n_v-1, n_v-1} & \mathbf{0}_{n_v-1} \\ (\Delta \omega_{\mathbf{r}}^{\xi})^T & \mathbf{0}_{n_v-1}^T & 0 \end{bmatrix};$$

$\mathbf{M}$  is a square matrix with dimensions  $(n_r + n_v) \times (n_r + n_v)$ , here  $n_r$  and  $n_v$  are the numbers of edges and vertices of the graph  $\mathbf{G}$ , accordingly;  $\Delta \omega_{\mathbf{r}}^{\xi}$  is the column vector of sectorial coordinates increments  $\Delta \omega_{\mathbf{r}}^{\xi} = \{\Delta \omega_{\mathbf{r},j}^{\xi} | j = \overline{1, n_r}\}^T$  consisting of  $n_r$  components calculated according to (2.3);  $\vec{S}_y$ ,  $\vec{S}_z$ ,  $\vec{S}_{\overline{\omega}}$  are the column vectors (3.16) with  $n_r$  components calculated according to (3.17), (3.18) and (3.19) respectively;  $\vec{S}_{hy}$ ,  $\vec{S}_{hz}$ ,  $\vec{S}_{h\overline{\omega}}$  are the column vectors (3.11)



with  $n_r$  components calculated according to (3.8), (3.9) and (3.10) respectively;  $S_{\rho y}$ ,  $S_{\rho z}$ ,  $S_{\rho \omega}$  are the integral section properties calculated according to (3.28), (3.29) and (3.30) respectively.

The solution of the system of equations (3.36) determines the column vector of shear forces flows  $\vec{T}_S = \{T_{S,j}\}^T, j = \overline{1, n_r}$ , at the start points of unbranched cross-section parts. The vector  $\vec{T}_S$  can be also presented as follow:

$$\vec{T}_S = M_x \vec{b}_x + \frac{Q_y}{I_z} \vec{b}_z + \frac{Q_z}{I_y} \vec{b}_y + \frac{M_{\omega}}{I_{\omega}} \vec{b}_{\omega}. \tag{3.37}$$

In this case, the system of algebraic equations (3.36) disintegrates and transforms into four systems of  $n_r + n_v$  algebraic equations relating to the column vectors  $\vec{b}_x, \vec{b}_y, \vec{b}_z$  and  $\vec{b}_{\omega}$  consisting of  $n_r$  elements [3] as presented below:

$$\mathbf{M} \times \begin{bmatrix} \vec{b}_x \\ \vec{\lambda}_x \\ \lambda_{n_x,x} \end{bmatrix} = \begin{bmatrix} \mathbf{0}_{n_r} \\ \mathbf{0}_{n_v-1} \\ 1 \end{bmatrix}; \quad \mathbf{M} \times \begin{bmatrix} \vec{b}_y \\ \vec{\lambda}_y \\ \lambda_{n_y,y} \end{bmatrix} = \begin{bmatrix} \frac{\vec{S}_{hy}}{G} \\ (\mathbf{i}' - |\mathbf{i}'|) \times \vec{S}_y \\ S_{\rho y} \end{bmatrix};$$

$$\mathbf{M} \times \begin{bmatrix} \vec{b}_z \\ \vec{\lambda}_z \\ \lambda_{n_z,z} \end{bmatrix} = \begin{bmatrix} \frac{\vec{S}_{hz}}{G} \\ (\mathbf{i}' - |\mathbf{i}'|) \times \vec{S}_z \\ S_{\rho z} \end{bmatrix}; \quad \mathbf{M} \times \begin{bmatrix} \vec{b}_{\omega} \\ \vec{\lambda}_{\omega} \\ \lambda_{n_{\omega},\omega} \end{bmatrix} = \begin{bmatrix} \frac{\vec{S}_{h\omega}}{G} \\ (\mathbf{i}' - |\mathbf{i}'|) \times \vec{S}_{\omega} \\ S_{\rho \omega} \end{bmatrix}, \tag{3.38}$$

where  $\vec{\lambda}_x = \{\lambda_{x,f}\}^T, \vec{\lambda}_y = \{\lambda_{y,f}\}^T, \vec{\lambda}_z = \{\lambda_{z,f}\}^T, \vec{\lambda}_{\omega} = \{\lambda_{\omega,f}\}^T, f = \overline{1, n_v - 1}$  are the unknown column vectors of Lagrange multipliers consisting of  $n_v - 1$  elements;  $\lambda_{n_x,x}, \lambda_{n_y,y}, \lambda_{n_z,z}, \lambda_{n_{\omega},\omega}$  are the additional Lagrange multipliers.

The projection of the vector  $\vec{b}_x = \{b_{x,j} | j = \overline{1, n_r}\}$  defined of the set of  $n_r$  unbranched sectional parts into the set of sectional segments  $\vec{b}_x^{\zeta} = \{b_{x,\kappa}^{\zeta} | \kappa = \overline{1, n_{\zeta} - 1}\}$  can be written as:  $b_{x,\kappa}^{\zeta} = b_{x,j} \quad \forall \kappa: \vec{s}_{\kappa}^{\zeta} \subseteq \mathbf{R}_j^{\zeta}$ ; and  $b_{x,\kappa}^{\zeta} = 0 \quad \forall \kappa: \vec{s}_{\kappa}^{\zeta} \cap \mathbf{R}_j^{\zeta} = \emptyset$ . Similarly, the column vectors  $\vec{b}_y = \{b_{y,j} | j = \overline{1, n_r}\}, \vec{b}_z = \{b_{z,j} | j = \overline{1, n_r}\}$  and  $\vec{b}_{\omega} = \{b_{\omega,j} | j = \overline{1, n_r}\}$  can be also projected into the set of sectional segments obtaining corresponded column vectors  $\vec{b}_y^{\zeta} = \{b_{y,\kappa}^{\zeta} | \kappa = \overline{1, n_{\zeta} - 1}\}, \vec{b}_z^{\zeta} = \{b_{z,\kappa}^{\zeta} | \kappa = \overline{1, n_{\zeta} - 1}\}$  and  $\vec{b}_{\omega}^{\zeta} = \{b_{\omega,\kappa}^{\zeta} | \kappa = \overline{1, n_{\zeta} - 1}\}$ .

The following transformations for the first moments of inertia and for the sectorial moment of inertia should be performed,  $\forall \kappa = \overline{1, n_{\zeta} - 1}$ :

$$\vec{S}_{oz,\kappa}^{\zeta} \leftarrow \{S_{oz,\kappa}^{\zeta} - b_{z,\kappa}^{\zeta}\}; \quad \vec{S}_{oy,\kappa}^{\zeta} \leftarrow \{S_{oy,\kappa}^{\zeta} - b_{y,\kappa}^{\zeta}\}; \tag{3.39}$$

$$\bar{S}_{o\bar{w},\kappa}^{\zeta} \leftarrow \left\{ S_{o\bar{w},\kappa}^{\zeta} - b_{\bar{w},\kappa}^{\zeta} \right\}; \quad \tilde{S}_{o\bar{w},\kappa}^{\zeta} \leftarrow \left\{ \bar{S}_{o\bar{w},\kappa}^{\zeta} - a_{\kappa}^{\zeta} \frac{I_{\bar{w}}}{\Omega_0} \right\}. \quad (3.40)$$

Let us define the sets of shear forces flows values for the start, middle and end points at the middle line of the sectional segments  $\mathbf{T}^{\zeta, st} = \left\{ T_{\kappa}^{\zeta, st} \right\}$ ,  $\mathbf{T}^{\zeta, mid} = \left\{ T_{\kappa}^{\zeta, mid} \right\}$ ,  $\mathbf{T}^{\zeta, end} = \left\{ T_{\kappa}^{\zeta, end} \right\}$ ,  $\kappa = \overline{1, n_{\zeta} - 1}$ , consisting of  $n_{\zeta} - 1$  elements (by the number of sectional segments) as presented below [16]:

$$T_{\kappa}^{\zeta, start} = \frac{\wp H}{\Omega_0} a_{\kappa}^{\zeta} - \frac{Q_y}{I_z} \bar{S}_{oz, \kappa}^{\zeta, start} - \frac{Q_z}{I_y} \bar{S}_{oy, \kappa}^{\zeta, start} - \frac{M_{\bar{w}}}{I_{\bar{w}}} \tilde{S}_{o\bar{w}, \kappa}^{\zeta, start}, \quad (3.41)$$

$$T_{\kappa}^{\zeta, mid} = \frac{\wp H}{\Omega_0} a_{\kappa}^{\zeta} - \frac{Q_y}{I_z} \bar{S}_{oz, \kappa}^{\zeta, mid} - \frac{Q_z}{I_y} \bar{S}_{oy, \kappa}^{\zeta, mid} - \frac{M_{\bar{w}}}{I_{\bar{w}}} \tilde{S}_{o\bar{w}, \kappa}^{\zeta, mid}, \quad (3.42)$$

$$T_{\kappa}^{\zeta, end} = \frac{\wp H}{\Omega_0} a_{\kappa}^{\zeta} - \frac{Q_y}{I_z} \bar{S}_{oz, \kappa}^{\zeta, end} - \frac{Q_z}{I_y} \bar{S}_{oy, \kappa}^{\zeta, end} - \frac{M_{\bar{w}}}{I_{\bar{w}}} \tilde{S}_{o\bar{w}, \kappa}^{\zeta, end}, \quad (3.43)$$

where the first moments of inertia  $\bar{S}_{oz, \kappa}^{\zeta}$ ,  $\bar{S}_{oy, \kappa}^{\zeta}$  and the sectorial moment of inertia  $\tilde{S}_{o\bar{w}, \kappa}^{\zeta}$  are calculated using transformations (3.39) and (3.40), accordingly.

The shear stresses for each  $\kappa^{\text{th}}$  sectional segment  $\boldsymbol{\tau}^{\zeta} = \left\{ \boldsymbol{\tau}_{\kappa}^{\zeta} = \left\{ \tau_{\kappa}^{\zeta, start}, \tau_{\kappa}^{\zeta, mid}, \tau_{\kappa}^{\zeta, end} \right\} \right\}$ ,  $\kappa = \overline{1, n_{\zeta} - 1}$ , can be calculated as presented below:

$$\boldsymbol{\tau}_{\kappa}^{\zeta} = \left\{ \begin{array}{l} \tau_{\kappa}^{\zeta, start} = \left| \frac{T_{\kappa}^{\zeta, start}}{\delta_{\kappa}^{\zeta}} \right| \pm \frac{(1 - \wp) H \delta_{\kappa}^{\zeta}}{I_k} \\ \tau_{\kappa}^{\zeta, mid} = \left| \frac{T_{\kappa}^{\zeta, mid}}{\delta_{\kappa}^{\zeta}} \right| \pm \frac{(1 - \wp) H \delta_{\kappa}^{\zeta}}{I_k} \\ \tau_{\kappa}^{\zeta, end} = \left| \frac{T_{\kappa}^{\zeta, end}}{\delta_{\kappa}^{\zeta}} \right| \pm \frac{(1 - \wp) H \delta_{\kappa}^{\zeta}}{I_k} \end{array} \right\}, \quad (3.44)$$

where the torsion moment of inertia  $I_x$  and the parameter  $\wp$  are calculated as:

$$I_x = I_k + I_{\Gamma} = \frac{1}{3} \sum_{\kappa=1}^{n_{\zeta}-1} I_{\kappa}^{\zeta} \left( \delta_{\kappa}^{\zeta} \right)^3 + I_{\Gamma}, \quad (3.45)$$

$$\wp = 1 - I_k / I_x. \quad (3.46)$$

The components  $\left| T_{\kappa}^{\zeta, start} / \delta_{\kappa}^{\zeta} \right|$ ,  $\left| T_{\kappa}^{\zeta, mid} / \delta_{\kappa}^{\zeta} \right|$  and  $\left| T_{\kappa}^{\zeta, end} / \delta_{\kappa}^{\zeta} \right|$  in (3.44) define shear stresses values for the start, middle and end points at the middle line of  $\kappa^{\text{th}}$  sectional segment, accordingly. Besides, transition from the shear stresses related to the middle line of  $\kappa^{\text{th}}$  segment to the shear stresses at the outside longitudinal edges of this segment can be performed by addition or subtraction of the member  $(1 - \wp) H \delta_{\kappa}^{\zeta} I_k^{-1}$ .

**5. Software implementation and numerical examples.** The numerical algorithm developed and presented above has been implemented in SCAD Office environment by the program TONUS ([www.scadsoft.com](http://www.scadsoft.com)) (see Fig. 5) [19]. The

computer program TONUS presented below is intended to create cross-sections of the thin-walled bars, to calculate geometrical properties as well as to calculate normal, shear and equivalent stresses in these cross-sections [5]. Software TONUS allows to consider arbitrary (including open-closed) cross-sections of the thin-walled bars. A cross-section of the thin-walled bar is constructed from the set of segments (stripes) by specifying node coordinates which define the position of segment ends as well as by specifying thicknesses for all segments.

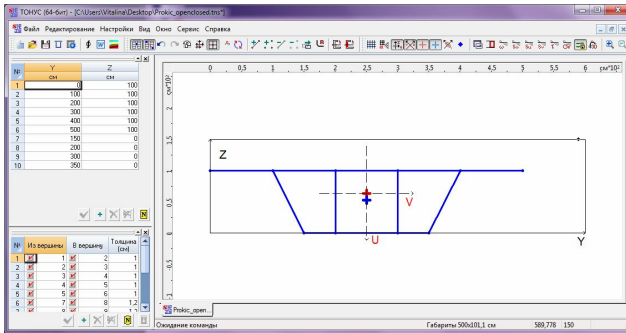


Fig. 5. TONUS main window

Besides calculation of geometrical properties for the cross-sections of the thin-walled bars software TONUS also represents sectorial coordinates diagram as well as static moment diagrams  $S_u$ ,  $S_v$  and first sectorial moment  $S_\omega$  diagram.

In order to represent normal, shear and equivalent stresses diagram in the section of the thin-walled bar user should specify internal forces acting in the section. Initial data to construct normal stresses diagram are bending moments  $M_u$  and  $M_v$  relating to the main axis of inertia of the thin-walled bar cross-section, axial force  $N$  applied at the center of mass of the section as well as warping bimoment  $B$ . Initial data to construct shear stresses diagram are shear forces  $Q_u$  and  $Q_v$  applied at the center of mass of the cross-section as well as total torque  $M_x$  and warping torque  $M_\omega$ . In order to represent equivalent stresses diagram user should also specify a strength theory.

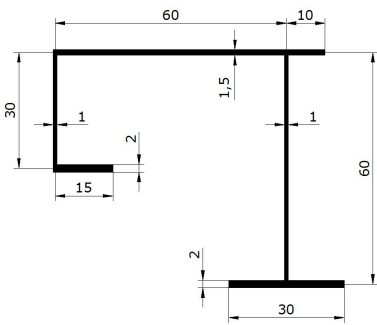


Fig. 6. Open section of thin-walled bar with cross-sectional sizes, cm

**5.1. Example 1: thin-walled bar with open profile.** Let us to consider an example of calculation of a thin-walled bar with open profile in order to validate developed algorithm and verify calculation accuracy for sectorial cross-section properties and shear stresses caused by warping torsion.

Initial data for calculation are presented by Fig. 6. Results of calculation, namely sectorial coordinates diagram  $\omega$ ,  $\text{cm}^2$ , and shear stresses diagram related to the value of warping torque

$\tau_{\omega} M_{\omega}^{-1} \times 10^7 \text{ (cm}^{-3}\text{)}$  have been obtained in paper [12] and presented by Fig. 7.

Results of calculation, namely sectorial coordinates  $\omega$ , sectorial moment of inertia  $S_{\omega}$  and shear stresses  $\tau_{\omega}$  caused by the warping torque  $M_{\omega} = 10^7 \text{ kN cm}$ , have been also obtained using TONUS software and presented by Figs. 8 – 10.

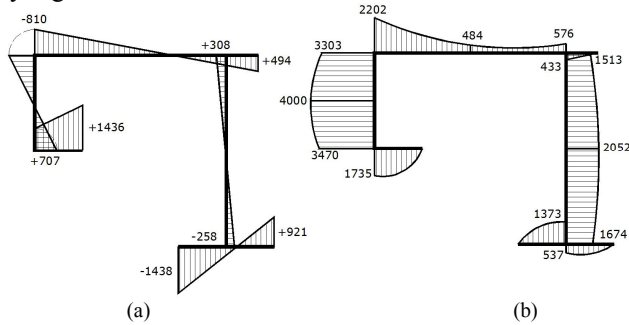


Fig. 7. Results of calculation according to [12]: (a) – sectorial coordinate diagram  $\omega$ ,  $\text{cm}^2$ ; (b) – shear stresses diagram related to the warping torque  $\tau_{\omega} M_{\omega}^{-1} \times 10^7$ ,  $\text{cm}^{-3}$

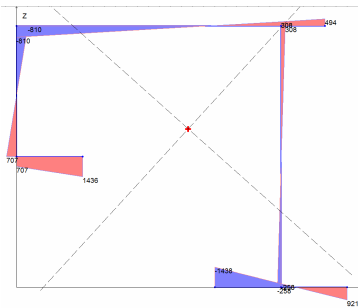


Fig. 8. Results of calculation obtained using TONUS software – sectorial coordinated diagram  $\omega$ ,  $\text{cm}^2$

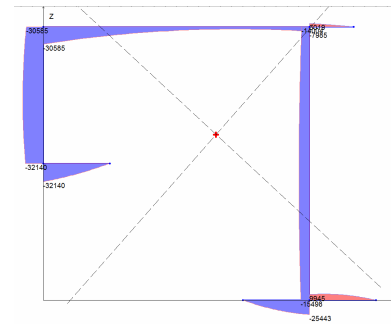


Fig. 9. Results of calculation obtained using TONUS software – sectorial moment of inertia  $S_{\omega}$ ,  $\text{cm}^4$

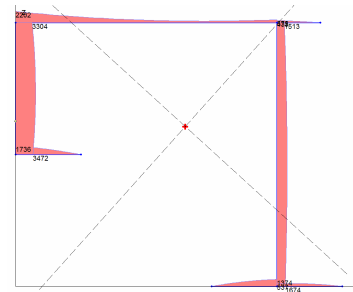


Fig. 10. Results of calculation obtained using TONUS software – modulus of shear stresses diagram  $\tau_{\omega}$  caused by warping torsion for the value of warping torque  $M_{\omega} = 10^7 \text{ kNcm}$ ,  $\text{kN/cm}^2$

Comparison for calculation results of sectorial first moment of inertia and shear stresses caused by warping torsion as well as comparison for calculation results of sectorial coordinates for considered cross-section of the thin-walled bar are presented by Tab. 1 and Tab. 2. As you can see deviations do not exceed 0,25% in all cases. It proves the validity of the results obtained using developed software.

Table 1

Comparison for calculation results of the first sectorial moment and shear stresses caused by the warping torque for considered open cross-section of the thin-walled bar

Section segment	Section point number	First sectorial moment $S_{\omega}$ , $\text{cm}^4$			Shear stresses $\tau_{\omega}$ , $\text{kN/cm}^2$ (when $M_{\omega} = 10^7$ , $\text{kNcm}$ )		
		[12]	TONUS	Deviation, %	[12]	TONUS	Deviation, %
1	1	32126	32140	0,04	1735	1736	0,06
1	2	0	0	0	0	0	0
2	1	32126	32140	0,04	3470	3472	0,06
2	8	30580	30585	0,02	3303	3304	0,06
3	8	30580	30585	0,02	2202	2202	0
3	4	7999	7985	0,18	576	575	0,17
4	4	6013	6019	0,1	433	432	0,23
4	5	0	0	0	0	0	0
5	4	14008	14004	0,03	1513	1513	0
5	3	15498	15498	0	1674	1674	0
6	6	0	0	0	0	0	0
6	3	25423	25443	0,08	1373	1374	0,07
7	3	9943	9945	0,02	537	537	0
7	7	0	0	0	0	0	0

Table 2

Comparison for calculation results of sectorial coordinates for considered open cross-section of the thin-walled bar

Section point number	Sectorial coordinate $\omega$ , $\text{cm}^2$		
	[12]	TONUS	Deviation, %
1	707	707	0
2	1436	1436	0
3	-258	-258	0
4	308	308	0
5	494	494	0
6	-1438	-1438	0
7	921	921	0
8	-810	-810	0

### 5.2. Example 2: thin-walled bar with open-closed multi-contour profile.

Let us to consider an example of calculation of a thin-walled bar with open-closed multi-contour profile in order to validate developed algorithm and verify calculation accuracy for geometrical cross-section properties and shear stresses caused by warping torsion as well as shear force. Initial data for calculation are presented by Fig. 11.

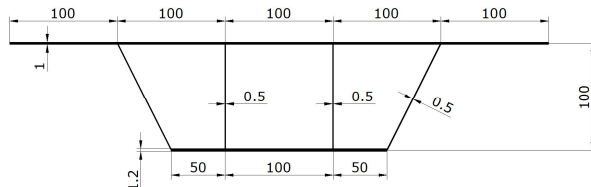


Fig. 11. Open-closed multi-contour section of the thin-walled bar with cross-sectional dimensions, cm

Calculation results, namely sectorial coordinates diagram  $\bar{\omega}$ , diagram of shear stresses caused by warping torsion related to the value of warping torque  $\tau_{\bar{\omega}} M_{\bar{\omega}}^{-1} \times 10^7$ , as well as diagram of shear stresses caused by acting of shear force related to the value of shear force  $\tau_u Q_u^{-1} \times 10^5$  have been obtained by Prokić [12] and presented by Fig. 12.

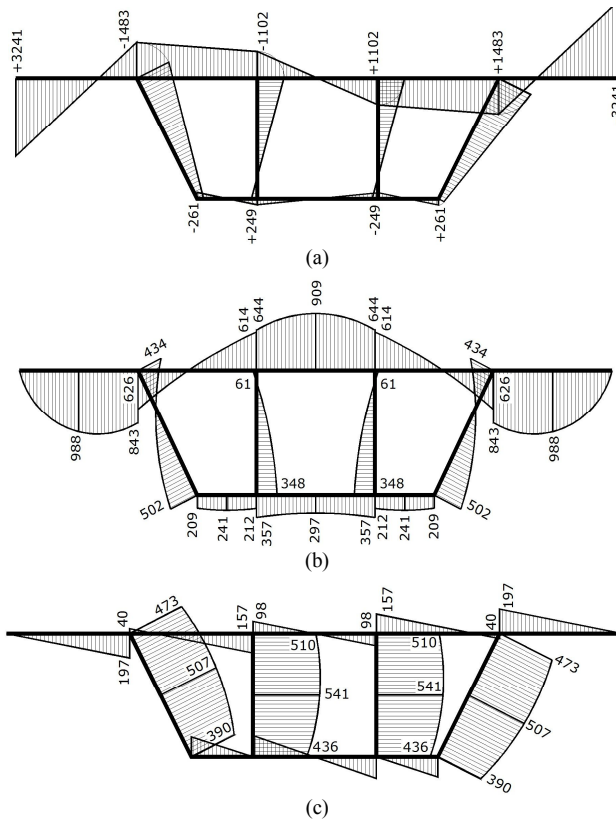


Fig. 12. Results of calculations according to [12]: (a) – sectorial coordinates diagram  $\bar{\omega}$ ,  $\text{cm}^2$ ; (b) – shear stresses diagram caused by warping torsion related to the value of the warping torque  $\tau_{\bar{\omega}} M_{\bar{\omega}}^{-1} \times 10^7$ ,  $\text{cm}^{-3}$ ; (c) – shear stresses diagram caused by shear force related to the value of shear force  $\tau_u Q_u^{-1} \times 10^5$ ,  $\text{cm}^{-2}$

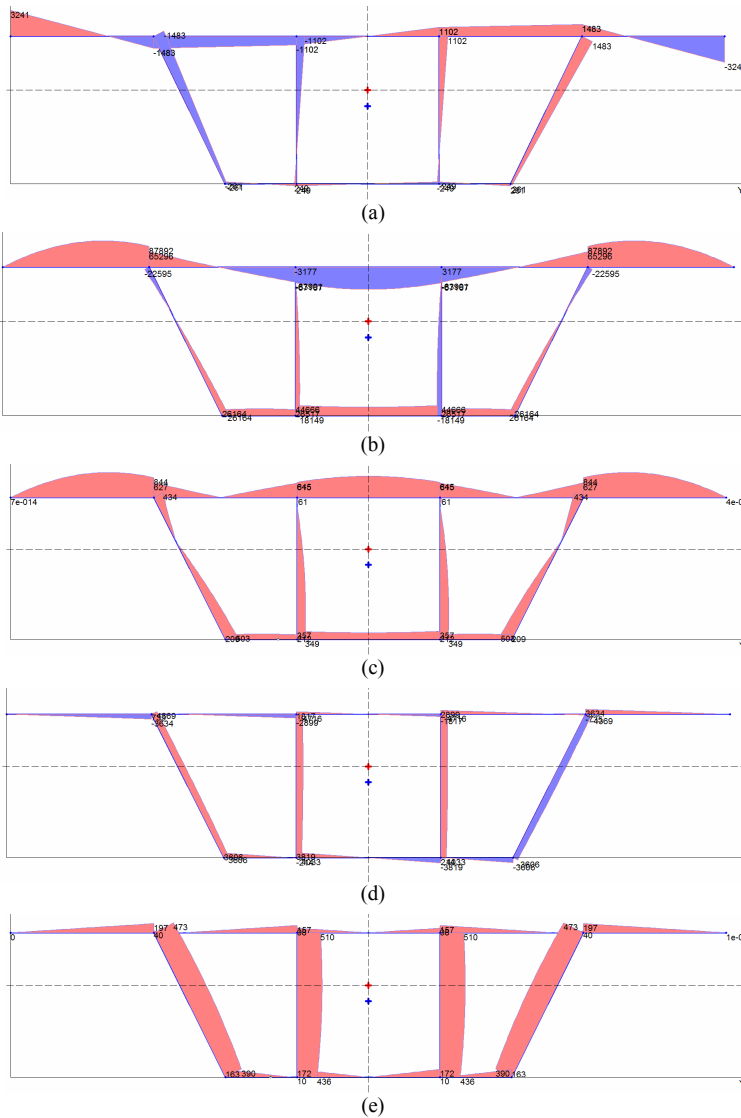


Fig. 13. Distribution diagrams obtained using TONUS software:

(a) – normalized sectorial coordinates  $\varpi$ , cm<sup>2</sup>;

(b) – first sectorial moment  $S_{\varpi}$ , cm<sup>4</sup>;

(c) – modulus of shear stresses  $\tau_{\varpi}$ , constructed depending on the value of the warping torque

$$M_{\varpi} = 10^7 \text{ kN cm, kN/cm}^2;$$

(d) – the first moment  $S_v$  relating to the principle axis  $v-v$ , cm<sup>3</sup>;

(e) – modulus of shear stresses  $\tau_u$ , constructed depending on the value of shear

$$\text{force } Q_u = 10^5 \text{ kN, kN/cm}^2$$

Table 3

Comparison for calculation results of first moments for considered open-closed multi-contour cross-section of the thin-walled bar

Section segment number	Section point number	First sectorial moment $S_{\sigma}$ , $\text{cm}^4$			First moment $S_y$ , $\text{cm}^3$		
		[12]	TONUS	Deviation, %	[12]	TONUS	Deviation, %
1	1	0	0	0	0	0	0
1	2	87776	87892	0,13	3643	3634	0,25
2	2	65181	65296	0,18	740	741	0,14
2	3	63932	64036	0,16	2903	2899	0,14
3	3	67055	67159	0,16	1812	1817	0,28
6	7	26114	26164	0,19	3595	3606	0,3
6	8	26489	26517	0,11	–	10	–
7	8	44606	44666	0,13	3816	3819	0,08
9	2	22595	22595	0	4373	4369	0,09
9	7	26135	26164	0,11	3606	3606	0
10	3	3176	3177	0,03	4715	4716	0,02
10	8	18117	18149	0,15	4031	4033	0,05

Table 4

Comparison for calculation results of shear stresses caused by the warping torque as well as by the shear force for considered open-closed multi-contour cross-section of the thin-walled bar

Section segment number	Section point number	Shear stresses $\tau_{\sigma}$ , $\text{kN/cm}^2$ (when $M_{\sigma} = 10^7$ , $\text{kNcm}$ )			Shear stresses $\tau_u$ , $\text{kN/cm}^2$ (when $Q_u = 10^5$ , $\text{kN}$ )		
		[12]	TONUS	Deviation, %	[12]	TONUS	Deviation, %
1	1	0	0	0	0	0	0
1	2	843	844	0,12	197	197	0
2	2	626	627	0,16	40	40	0
2	3	614	615	0,16	157	157	0
3	3	644	645	0,16	98	98	0
6	7	209	209	0	162	163	0,6
6	8	212	212	0	–	10	0
7	8	357	357	0	172	172	0
9	2	434	434	0	473	473	0
9	7	502	503	0,20	390	390	0
10	3	61	61	0	510	510	0
10	8	348	349	0,29	436	436	0



Table 5

Comparison for calculation results of normalized sectorial coordinate for considered open-closed multi-contour cross-section of the thin-walled bar

Section point number	Sectorial coordinate $\varpi$ , cm <sup>2</sup>		
	[12]	TONUS	Deviation, %
1	+3241	+3241	0
2	-1483	-1483	0
3	-1102	-1102	0
7	-261	-261	0
8	+249	+249	0

Calculation results, namely sectorial coordinates  $\varpi$ , static moment  $S_v$  relating to the main axes of inertia  $v-v$ , first sectorial moment  $S_{\varpi}$ , shear stresses  $\tau_u$  caused by shear force  $Q_u = 10^5$  kN as well as shear stresses  $\tau_{\varpi}$  caused by warping torque  $M_{\varpi} = 10^7$  kNcm for considered open-closed multi-contour section of the thin-walled bar have been obtained using TONUS software and presented by Fig. 13.

Comparison for calculation results of first moment  $S_v$  and first sectorial moment  $S_{\varpi}$ , comparison for calculation results of shear stresses  $\tau_u$  and  $\tau_{\varpi}$  caused by shear force  $Q_u$  and warping torque  $M_{\varpi}$  respectively as well as comparison for calculation results of sectorial coordinates  $\varpi$  for considered open-closed multi-contour cross-section of the thin-walled bar are presented by Tabs. 3 – 5. Deviations are no more than 0,3% in all design cases. It proves the validity of the results obtained using developed software.

**Conclusions.** The searching problem of shear stresses outside longitudinal edges of an arbitrary cross-section (including open-closed multi-contour cross-sections) of a thin-walled bar subjected to the general load case has been considered in the paper. The formulated problem has been transformed into a minimization problem of Castigliano's functional subject to constraints-equalities of shear forces flows equilibrium formulated for cross-section branch points as well as subject to an equilibrium equation for the whole cross-section relating to longitudinal axes of the thin-walled bar.

A detailed numerical algorithm intended to solve searching problem of shear forces flows for an arbitrary cross-section of a thin-walled bar subjected to the general loading case using the mathematical apparatus of the graph theory has been developed. The algorithm is oriented on software implementation in systems of computer-aided design of thin-walled bar structures. Developed algorithm has been implemented in SCAD Office environment by the program TONUS.

Numerical examples for calculation of the thin-walled bars with open and open-closed multi-contour cross-sections have been considered in order to validate developed algorithm and verify calculation accuracy for sectorial cross-section geometrical properties and shear stresses caused by warping torque and shear forces. Validity of the calculation results obtained using developed software has been proven by considered examples.

## REFERENCES

1. *Robert K. Dowell, Timothy P. Johnson*. Closed-form shear flow solution for box-girder bridges under torsion // *Engineering Structures*. – No. 34, 2012. – p. 383–390.
2. *Perelmuter A. V., Slivker V. I.* Numerical structural analysis: models, methods and pitfalls. – Springer-Verlag Berlin Heidelberg, 2003. – 600 p.
3. *Slivker V. I.* Mechanics of structural elements. Theory and applications. – Springer-Verlag Berlin Heidelberg, 2007. – 786 p.
4. *Lalin V. V., Rybakov V. A., Diakov S. F., Kudinov V. V., Orlova E. S.* The semi-shear theory of V. I. Slivker for the stability problems of thin-walled bars // *Magazine of Civil Engineering*. – Vol. 87, Issue 3, 2019. – p. 66–79.
5. *Yurchenko V. V.* Proyektirovaniye karkasov zdaniy iz tonkostennykh kholodnogutykh profiley v srede SCAD Office [Designing of steel frameworks from thin-walled cold-formed profiles in SCAD Office] // *Magazine of Civil Engineering*. – No. 8, 2010. – p. 38–46. (rus)
6. *Jönsson J.* Determination of shear stresses, warping functions and section properties of thin-walled beams using finite elements // *Computer and Structures*. – No. 68, 1998. – p. 393–410.
7. *Tarjan R.* Depth-first search and linear graph algorithms // *SIAM Journal Computing*. – No. 1, 1972. – p. 146–60.
8. *Alfano G., Marotti de Sciarra F., Rosati L.* Automatic analysis of multicell thin-walled sections // *Computer and Structures*. – No. 59, 1996. – p. 641–655.
9. *Waldron P.* Sectorial properties of straight thin-walled beams // *Computers and Structures*. – Vol. 24, Issue 1, 1986. – p. 147–156.
10. *Yoo C. H.* Cross-sectional properties of thin-walled multi-cellular section // *Computer and Structures*. – No. 22, 1986. – p. 53–61.
11. *Chai H. Yoo, Junsuk Kang, Kyungsik Kim, Kyoung C. Lee.* Shear flow in thin-walled cellular sections // *Thin-Walled Structures*. – No. 49 (11), 2011. – p. 1341–1347.
12. *Prokić A.* Computer program for determination of geometrical properties of thin-walled beams with open-closed section // *Computers and Structures*. – No. 74, 2000. – p. 705–715.
13. *Gurujee C. S., Shah K. R.* A computer program for thin-walled frame analysis // *Advances in Engineering Software*. – No. 11, 1989. – p. 58–70.
14. *Gajanan K. Choudhary, Karan M. Doshi.* An algorithm for shear stress evaluation in ship hull girders // *Ocean Engineering*. – No. 108 (1), 2015. – p. 678–691.
15. *Perelmuter A., Yurchenko V.* Shear stresses in hybrid thin-walled section: development of detail numerical algorithm based on the graph theory // *Proceedings of 3<sup>rd</sup> Polish Congress of Mechanics and 21<sup>st</sup> International Conference on Computer Methods in Mechanics. Short Papers*. – Vol. 2, 2015. – p. 943–944.
16. *Yurchenko V.* Searching shear forces flows for an arbitrary cross-section of a thin-walled bar: development of numerical algorithm based on the graph theory // *International journal for computational civil and structural engineering*. – No. 15(1), 2019. – p. 153–170.
17. *Yurchenko V. V.* Rozpodil potokiv dotychnykh zusyly vzdovzh zamknytykh konturiv pererizu tonkostinnoho sterzhnia: rozrobka chyslovoho alhorytmu z vykorystanniam teorii hrafiv [Distribution of shear forces flows along closed contours of a thin-walled bar section: development of numerical algorithm based on the graph theory] // *Resursoekonomni materialy, konstruktzii, budivli ta sporudy* [Resource-economic materials, structural members, buildings and structures]. Collected scientific articles. Issue 30. – Rivne, 2015. – p. 306–316. (ukr)
18. *Yurchenko V. V.* Uzahalneni sektorialni koordynaty dlia dovilnoho pererizu tonkostinnoho sterzhnia: rozrobka chyslovoho alhorytmu z vykorystanniam teorii hrafiv [Normalized sectorial coordinates for an arbitrary cross-section of a thin-walled bar: development of numerical algorithm based on the graph theory] // *Resursoekonomni materialy, konstruktzii, budivli ta sporudy* [Resource-economic materials, structural members, buildings and structures]. Collected scientific articles. Issue 31. – Rivne, 2015. – p. 538–549. (ukr)
19. *Rud' D. N., Yurchenko V. V.* Prohrammaia realizatsiya poyska potokov kasatelynykh usylii v secheny tonkostennogo sterzhnia proyvolnoi konfyhurasyy [Software implementation of searching for shear forces flows for an arbitrary cross-section of a thin-walled bar] // *Suchasni metody i problemno-orientovani kompleksy rozrakhunku konstruktzii i yikh zastosuvannia u proektuvanni i navchalnomu protsesi* [Modern methods and problem-oriented structural analysis complexes and its application in design and training]: proceedings of second international scientific and practical conference, Kyiv, 2018. – p. 109–111. (rus)

## СПИСОК ЛІТЕРАТУРИ

1. *Dowell R. K., Johnson T. P.* Closed-form shear flow solution for box–girder bridges under torsion // *Engineering Structures*. – №34, 2012. – p. 383–390.
2. *Perelmuter A. V., Slivker V. I.* Numerical structural analysis: models, methods and pitfalls. – Springer-Verlag Berlin Heidelberg, 2003. – 600 p.
3. *Slivker V. I.* Mechanics of structural elements. Theory and applications. – Springer-Verlag Berlin Heidelberg, 2007. – 786 p.
4. *Lalin V. V., Rybakov V. A., Diakov S. F., Kudinov V. V., Orlova E. S.* The semi-shear theory of V. I. Slivker for the stability problems of thin-walled bars // *Magazine of Civil Engineering*. – № 87(3), 2019. – С. 66 – 79.
5. *Юрченко В. В.* Проектирование каркасов зданий из тонкостенных холодногнутых профилей в среде SCAD Office // *Magazine of Civil Engineering*. – №8, 2010. – С. 38 – 46.
6. *Jönsson J.* Determination of shear stresses, warping functions and section properties of thin-walled beams using finite elements // *Computer and Structures*. – No. 68, 1998. – p. 393–410.
7. *Tarjan R.* Depth-first search and linear graph algorithms // *SIAM Journal Computing*. – №1, 1972. – p. 146 – 60.
8. *Alfano G., Marotti de Sciarra F., Rosati L.* Automatic analysis of multicell thin-walled sections // *Computer and Structures*. – №59, 1996. p. 641 – 55.
9. *Waldron P.* Sectorial properties of straight thin-walled beams // *Computers and Structures*. – Vol. 24, Issue 1, 1986. – p. 147 – 156.
10. *Yoo C. H.* Cross-sectional properties of thin-walled multi-cellular section // *Computer and Structures*. – №22, 1986. – p. 53–61.
11. *Chai H.Yoo, Junsuk Kang, Kyungsik Kim, Kyoung C. Lee.* Shear flow in thin-walled cellular sections // *Thin-Walled Structures*. – №49 (11), 2011. – p. 1341–1347.
12. *Prokić A.* Computer program for determination of geometrical properties of thin-walled beams with open-closed section // *Computers and Structures*. – №74, 2000. – p. 705–715.
13. *Gurujee C. S., Shah K. R.* A computer program for thin-walled frame analysis // *Advances in Engineering Software*. – No. 11, 1989. – p. 58 – 70.
14. *Gajanan K.Choudhary, Karan M. Doshi.* An algorithm for shear stress evaluation in ship hull girders // *Ocean Engineering*. – №108 (1), 2015. – p. 678–691.
15. *Perelmuter A., Yurchenko V.* Shear stresses in hybrid thin-walled section: development of detail numerical algorithm based on the graph theory // *Proceedings of 3<sup>rd</sup> Polish Congress of Mechanics and 21<sup>st</sup> International Conference on Computer Methods in Mechanics. Short Papers*. – Vol. 2, 2015. – p. 943 – 944.
16. *Yurchenko V.* Searching shear forces flows for an arbitrary cross-section of a thin-walled bar: development of numerical algorithm based on the graph theory // *International journal for computational civil and structural engineering*. – №15(1), 2019. – p. 153 – 170.
17. *Юрченко В. В.* Розподіл потоків дотичних зусиль вздовж замкнених контурів перерізу тонкостінного стержня: розробка числового алгоритму з використанням теорії графів // *Ресурсоекономічні матеріали, конструкції, будівлі та споруди. Збірник наукових праць*. Вип. 30. – Рівне, 2015. – С. 306 – 316.
18. *Юрченко В. В.* Узагальнені секторіальні координати для довільного перерізу тонкостінного стержня: розробка числового алгоритму з використанням теорії графів // *Ресурсоекономічні матеріали, конструкції, будівлі та споруди. Збірник наукових праць*. Вип. 31. – Рівне, 2015. – С. 538 – 549.
19. *Рудь Д. Н., Юрченко В. В.* Программная реализация поиска потоков касательных усилий в сечении тонкостенного стержня произвольной конфигурации // *Сучасні методи і проблемно-орієнтовані комплекси розрахунку конструкцій і їх застосування у проектуванні і навчальному процесі: Тези доповідей другої міжнародної науково-практичної конференції, Київ, 2018.* – С. 109 – 111.

Стаття надійшла 21.08.2019

*Yurchenko V. V.*

### **SEARCHING FOR SHEAR FORCES FLOWS IN ARBITRARY CROSS-SECTIONS OF THIN-WALLED BARS: DEVELOPMENT OF NUMERICAL ALGORITHM**

Development of a general computer program for the design and verification of thin-walled bar structural members remains an actual task. Despite the prevailing influence of normal stresses on the stress-strain state of thin-walled bars design and verification of thin-walled structural members should be performed taking into account not only normal stresses, but also shear stresses.

Therefore, in the paper a thin-walled bar of an arbitrary cross-section which is undergone to the general load case is considered as investigated object. The main research question is development of mathematical support and knoware for numerical solution for the shear stresses problem with orientation on software implementation in a computer-aided design system for thin-walled bar structures.

The problem of shear stresses outside longitudinal edges of an arbitrary cross-section (including open-closed multi-contour cross-sections) of a thin-walled bar subjected to the general load case has been considered in the paper. The formulated problem has been reduced to the searching problem for unknown shear forces flows that have the least value of the Castigliano's functional. Besides, constraints-equalities of shear forces flows equilibrium formulated for cross-section branch points, as well as equilibrium equation formulated for the whole cross-section relating to longitudinal axes of the thin-walled bar have been taken into account.

A detailed numerical algorithm intended to solve the formulated problem has been proposed by the paper. The algorithm is oriented on software implementation in systems of computer-aided design of thin-walled bar structures. Developed algorithm has been implemented in SCAD Office environment by the program TONUS. Numerical examples for calculation of thin-walled bars with open and open-closed multi-contour cross-sections have been considered in order to validate developed algorithm and verify calculation accuracy for sectorial cross-section geometrical properties and shear stresses caused by warping torque and shear forces. Validity of the calculation results obtained using developed software has been proven by considered examples.

**Keywords:** thin-walled bar, arbitrary cross-section, shear forces flow, closed contour, graph theory, Castigliano's functional, mathematical programming task, method of Lagrange multipliers, algorithm, software implementation.

*Юрченко В. В.*

### **ПОШУКОВИЙ АЛГОРИТМ ВИЗНАЧЕННЯ ПОТОКІВ ДОТИЧНИХ ЗУСИЛЬ ДЛЯ ДОВІЛЬНОГО ПЕРЕРІЗУ ТОНКОСТІННОГО СТЕРЖНЯ**

Розробка універсального програмного комплексу для розрахунку та проектування тонкостінних стержневих елементів конструкцій наясодні залишається актуальною задачею. Не дивлячись на визначальний вплив нормальних напружень на напружено-деформований стан тонкостінних стержнів, перевірка несучої здатності таких елементів повинна виконуватись, беручи до уваги також і значення дотичних напружень.

У зв'язку з цим розглянута задача пошуку значень потоків дотичних зусиль для довільного перерізу (відкрито-замкнутого багатоконтурного) тонкостінного стержня для загального випадку навантаження. Сформульована задача зведена до задачі математичного програмування, а саме до задачі пошуку невідомих потоків дотичних напружень, що забезпечують найменше значення функціоналу Кастільяно при задоволенні обмежень рівноваги потоків у точках розгалуження перерізу, а також при задоволенні рівняння рівноваги усього перерізу тонкостінного стержня відносно поздовжньої осі.

Розроблений детальний алгоритм числового розв'язку сформульованої задачі з використанням математичного апарату теорії графів, орієнтований на програмну реалізацію в системах автоматизованого проектування тонкостінних стержневих систем. Виконана програмна реалізація розробленого алгоритму у середовищі обчислювального комплексу SCAD Office у програмі TONUS.

З метою верифікації розробленого алгоритму та перевірки точності обчислень геометричних характеристик перерізу та дотичних напружень у ньому розглянуті приклади розрахунку тонкостінних стержневих елементів відкритого та відкрито-замкнутого багатоконтурного перерізів. На розглянутих прикладах доведена достовірність результатів, отримуваних за допомогою розробленого програмного забезпечення.

**Ключові слова:** тонкостінний стержень, довільний переріз, потоки дотичних зусиль, замкнутий контур, теорія графів, функціонал Кастільяно, задача математичного програмування, метод множників Лагранжа, алгоритм, програмна реалізація.

Юрченко В. В.

### **ПОИСКОВЫЙ АЛГОРИТМ ОПРЕДЕЛЕНИЯ ПОТОКОВ КАСАТЕЛЬНЫХ УСИЛИЙ ДЛЯ ПРОИЗВОЛЬНЫХ СЕЧЕНИЙ ТОНКОСТЕННЫХ СТЕРЖНЕЙ**

Разработка универсального программного комплекса для расчета и проектирования тонкостенных стержневых элементов конструкций остается актуальной задачей. Несмотря на преобладающее влияние нормальных напряжений на напряженно-деформированное состояние тонкостенных стержней, проверка несущей способности таких элементов должна выполняться, принимая во внимание также и значения касательных напряжений.

В связи с этим рассмотрена задача поиска значений потоков касательных усилий для произвольного сечения (открыто-замкнутого многоконтурного сечения) тонкостенного стержня для общего случая нагружения. Сформулированная задача приведена к задаче математического программирования, а именно к задаче поиска значений неизвестных потоков касательных напряжений, обеспечивающих наименьшее значение функционала Кастильяно при удовлетворении ограничений равновесия потоков в точках ветвления сечения, а также при удовлетворении уравнения равновесия всего сечения тонкостенного стержня относительно продольной оси.

Разработан детальный алгоритм численного решения сформулированной задачи с использованием математического аппарата теории графов, ориентированный на программную реализацию в системах автоматизированного проектирования тонкостенных стержневых систем. Выполнена программная реализация разработанного алгоритма в среде вычислительного комплекса SCAD Office в программе ТОНУС.

С целью верификации разработанного алгоритма и проверки точности вычислений геометрических характеристик и касательных напряжений рассмотрены примеры расчета тонкостенных стержневых элементов открытого и открыто-замкнутого многоконтурного сечений. На рассмотренных примерах доказана достоверность результатов, получаемых при использовании разработанного программного обеспечения.

**Ключевые слова:** тонкостенный стержень, произвольное сечение, потоки касательных усилий, замкнутый контур, теория графов, функционал Кастильяно, задача математического программирования, метод множителей Лагранжа, алгоритм, программная реализация

УДК 624.014

*Юрченко В. В. Пошуковий алгоритм визначення потоків дотичних зусиль для довільного перерізу тонкостінного стержня та його програмна реалізація // Опір матеріалів і теорія споруд: наук.-тех. збірн. – К.: КНУБА, 2019. – Вип. 103. – С. 82–111.*

*Розглянута задача пошуку потоків дотичних зусиль у довільному перерізі тонкостінного стержня для загального випадку навантаження. Розроблений детальний алгоритм числового розв'язку сформульованої задачі та виконана його програмна реалізація. На розглянутих прикладах розрахунок тонкостінних стержневих елементів відкритого та відкрито-замкнутого багатоконтурного перерізу доведена достовірність результатів, отримуваних за допомогою розробленого програмного забезпечення.*

Лл. 13. Табл. 5. Бібліог. 19 назв.

UDC 624.014

*Yurchenko V. V. Searching for shear forces flows in arbitrary cross-sections of thin-walled bars: numerical algorithm and software implementation // Strength of Materials and Theory of Structures: Scientific-and-technical collected articles – Kyiv: KNUBA, 2019. – Issue 103. – P. 82–111.*

*The problem of shear stresses outside longitudinal edges of an arbitrary cross-section of a thin-walled bar subjected to the general load case has been considered. A detailed numerical algorithm intended to solve the formulated problem has been proposed and has been implemented by the software. Validity of the calculation results obtained using developed software has been proven by considered numerical examples for calculation of thin-walled bars with open and open-closed multi-contour cross-sections.*

Fig. 13. Tab. 5. Ref. 19.

УДК 624.014

*Юрченко В. В. Поисковый алгоритм определения потоков касательных усилий для произвольных сечений тонкостенных стержней и его программная реализация // Сопrotивление материалов и теория сооружений: науч.- тех. сборн. – К.: КНУСА, 2019. – Вып. 103. – С. 82–111.*

*Рассмотрена задача поиска потоков касательных усилий в произвольном сечении тонкостенного стержня для общего случая загрузки. Разработан детальный алгоритм численного решения сформулированной задачи и выполнена его программная реализация. На рассмотренных примерах расчета тонкостенных стержневых элементов открытого и открыто-замкнутого многоконтурного сечений доказана достоверность результатов, получаемых с использованием разработанного программного обеспечения.*

*Ил. 13. Табл. 5. Библиог. 19 назв.*

**Автор:** кандидат технічних наук, доцент кафедри металевих та дерев'яних конструкцій  
*Юрченко Віталіна Віталіївна*

**Адреса:** 03680 Україна, м. Київ, Повітрофлотський пр. 31, Київський національний університет будівництва і архітектури

**Робочий тел.:** +38(044)249-71-91

**Мобільний тел.:** +38(063)89-26-491

**Імейл:** [vitalina@scadsoft.com](mailto:vitalina@scadsoft.com)

**ORCID ID:** <https://orcid.org/0000-0003-4513-809X>